Sedimentology and Architecture of a Partially Contained Deposit, Cerro Solitario, Magallanes Basin, Chilean Patagonia

Sarah N. Jancuska

Thesis submitted to the faculty of the Virginia Polytechnic Institute and State University in partial fulfillment of the requirements for the degree of

Master of Science
In
Geosciences

Brian W. Romans, Chair
Benjamin C. Gill
Kenneth A. Eriksson

November 29, 2016
Blacksburg, VA

Keywords: Partially contained deposits, evolution of partial containment, fill-and-spill, seafloor topography, growth faulting, architecture of partially contained deposits, Magallanes Basin

Sedimentology and Architecture of a Partially Contained Deposit, Cerro Solitario, Magallanes Basin, Chilean Patagonia

Sarah N. Jancuska

Abstract

The depositional styles of sediment gravity currents depend, in part, on the relationship of flow magnitude to the scale of topographically controlled containment and range from unconfined lobes to fully contained deposits. Determining the degree of containment is important for understanding depositional processes, land to ocean sediment transfer and subsurface reservoir characterization/prediction. Depositional models of the fully contained (commonly referred to as "ponded") end member have been developed (e.g. fill-and-spill model). However, fully contained deposits represent only a portion of deepwater deposits and little work has been done identifying and examining the degree of containment of the more complex, partially contained deposits in outcrop.

Here, I document the sedimentological facies and stratigraphic architecture of the Zorrillo Unit, a partially contained system exposed at Cerro Solitario within the Upper Cretaceous Tres Pasos Formation of the Magallanes Basin. The evolution of partial containment at this outcrop is expressed as: 1) bypass in the proximal zone and flow stripping in the distal zone, 2) backstepping and blanketing of the outcrop, followed by 3) renewed bypass. The partially contained system at Cerro Solitario deviates from the widely used fill-and-spill model due to subtle relief. This record of infilling provides insight into the overall evolution of the depositional system. Within the Magallanes Basin, the partially contained and linked depocenters along the Chingue Clinoform represent the dying breaths of the Cerro Toro axial conglomerate channel system as the canyon-fed point source collapsed and choked off the sediment routing system out to the distal basin.

Sedimentology and Architecture of a Partially Contained Deposit, Cerro Solitario, Magallanes Basin, Chilean Patagonia

Sarah N. Jancuska

General Audience Abstract

Subaqueous sediment gravity flows are responsible for moving large quantities of sediment from off the continent to the oceanic abyssal plain and the resulting deposits serve as some of the largest hydrocarbon reservoirs in the world. These deposits vary in a number of ways depending on numerous variables, including containment. Containment is related to how the sediment gravity flows interact with the seafloor topography. Models have been created describing at one end of the spectrum sediment gravity flows that have been fully contained (i.e., the fill-and-spill model) where the flows are trapped and not able to escape the confining topography. The other end of the spectrum is where flows do not experience any containment (unconfined lobes). There is a lack of work done addressing the middle ground of partial containment of sediment gravity flows and their resulting deposits.

The Zorrillo Unit crops out at Cerro Solitario within the Late Cretaceous Magallanes Basin in southern Chile and offers a perfect location to study partially contained deposits. The architecture (the structure of the rocks) and facies (the character of the rocks) were identified. By characterizing and understanding the processes that created the partially contained outcrop, this outcrop can now be used as an analog for other similar depositional systems. Oil and gas companies use these outcrop analogs to aid in reservoir prediction for comparable deposition systems in the subsurface. Regionally, the context of the Zorrillo Unit within the Magallanes Basin is ambiguous and by characterizing it, details are added to this part of the basin's history.

Acknowledgements

None of this would have been possible without the guidance and support of my advisor, Brian Romans. Many thanks to him for taking a chance on me and introducing me to the wonderful world of deepwater depositional systems. My committee members are thanked for their time and feedback during the past two and a half years. My family has been incredibly supportive and encouraging throughout this processes and are always interested in hearing about what I am doing. Last but not least is the VT Seddies Group, an amazing group of people that have kept me sane during my time at VA Tech.

I would also like to thank Neal Auchter, Sarah Southern, Ben Daniels, Sebastian Kaempfe, Dan Niquet, Adam Nielson, Casey Meirovitz and Dan Hill for help with fieldwork. I also appreciate the insights and discussions with Steve Hubbard, Lisa Stright, Zane Jobe, Julia Fosdick and Per Pedersen along with many others who stopped by HTP throughout the field seasons. We also thank the land owners Don Raul Cardenez and Don Victor Hernadez for access to Cerro Solitario. Funding was provided by the Chile Slope Systems Joint Industry Project (CSS JIP) by our sponsors: Chevron, ConocoPhillips, Statoil, Shell, BG Group, Marathon Oil, Tailsman Energy, Anadarko, Hess, BP, BHP Billiton, Maersk, and Nexen.

CONTENTS

FIGURES

TABLES

1. Introduction

Interactions between seafloor topography and deep-marine sediment gravity flows result in a wide range of depositional features (Adeogba et al., 2005; Amy et al., 2007; Bersezio et al., 2005; Felletti, 2002; Gamberi and Rovere, 2011; Grecula et al., 2003; Haughton, 1994; Kneller et al., 1991; Kopriva and Kim, 2015; Li et al., 2012; Marchès et al., 2010; Prather et al., 1998; Sinclair and Tomasso, 2002; Spychala et al., 2015). The relief and geometry of the bounding topography are major controls on how contained a sediment gravity flow will be. If a flow is fully ponded, i.e., the confining topography does not allow any of the flow to escape and no flow stripping (*sensu* Piper and Normark, 1983) occurs, the flow is considered be fully contained. If deposition of the basal, coarser-grained part of the flow occurs simultaneously with flow stripping of the upper, finer-grained part of the flow, then partial containment of the flow occurs. The bypass of sediment results in major volumes of sediment being moved past a fixed geologic point and subsequently deposited basinward. Sediment gravity flows that have been fully contained have several defining characteristics that can be identified from preserved deposits, including: thick mud caps (Haughton, 1994; Patacci et al., 2015; Pickering and Hiscott, 1985; Sinclair and Tomasso, 2002), beds that lapout onto or pinch out towards an underlying surface (Haughton, 1994; Sinclair and Tomasso, 2002), flow reversals recorded in sedimentary structures (Haughton, 1994; Patacci et al., 2015; Pickering and Hiscott, 1985; Tinterri et al., 2016), and irregular underlying topography (Prather et al., 1998; Sinclair and Tomasso, 2002). These characteristics are used to describe full containment but this does not mean that they are exclusive to fully contained deposits. The range of containment results in various different expressions in the rock record. The

widely applied fill-and-spill model (Prather et al., 2012, 1998; Sinclair and Tomasso, 2002) has been proposed to explain the process and the depositional results of full containment. Sinclair and Tomasso (2002) synthesized seismic-reflection data and seafloor bathymetry with outcrop data from Tertiary Alpine Basins to create a fill-and-spill depositional model of a fully contained outcrop. It is broken up into four phases: 1) flow ponding, 2) flow stripping, 3) bypass and 4) blanketing. These fill-and-spill models result in a consistent stratigraphic pattern: thick sandstone-mudstone couplets in the phase 1, with the net-to-gross (i.e., sandstone-mudstone ratio) increasing as flow stripping occurs during the transition from phase 1 to phase 2. As the accommodation is filled during phase 2, the flows start to breach the bounding topography, which promotes incision and erosion at the spill point (where the flows exit the proximal sub-basin and spill over into the next sub-basin), ultimately resulting in bypass of the flows down dip into the next basin (phase 3). During phase 4, the flows fill that next sub-basin, they start to backfill where they had previously incised into the spill point resulting in a reduction in the slope gradient (Sinclair and Tomasso, 2002).

The conventional fill-and-spill model emphasizes full containment in the early stages of the model, which eventually results in a reduction of relief; however partial containment does not have the relief needed to fully contain flows in the early stages, resulting in bypass. Little has been done on outcrops to document the evolution of partially contained deposits due to the lack of criteria distinguishing them from fully contained. Partially contained deposits have been identified in seismic-reflection data of the Gulf of Mexico and they showed repeated patterns, or cycles, of high-energy processes (more chaotic) to lower-energy processes (more ordered) (Yeilding and Apps,

1994). This cyclicity and the processes that generate the cyclicity in what are interpreted as partially contained deposits by Yeilding and Apps (1994) has not been specifically addressed in outcrop studies.

The study interval represents a small part of the Magallanes Basin. Incorporating the Zorrillo Unit at Cerro Solitario into the regional stratigraphy will allow us to address regional correlations. The study interval sits at the transition between two deepwater depositional systems. The Chingue Clinoform, which the Zorrillo Unit marks the base of, has been mapped throughout the basin but its context within the basin is disputed. There are contrasting hypothesis relating to, which deepwater system the Zorrillo Unit is linked to. One idea is that the Zorrillo Unit is the distal equivalent to the overlying prograding slope system. Alternatively, the Zorrillo Unit is an overbank deposit of the underlying axial conglomeratic channel. By characterizing the outcrop we hope to shed new light on this transition and help constrain the larger regional evolution during this time.

The aim of this paper is to: 1) document facies and architecture of a 40-60 m thick turbiditic sandstone-rich package across a 3 km updip-to-downdip transect; 2) examine degrees of flow containment (ponding versus bypass) spatially across the outcrop belt and through stratigraphy within the context of the widely used fill-and-spill conceptual models; and 3) investigate regional correlations and discuss basin-scale controls on the submarine depositional environment.

2. Geologic Setting

The Magallanes Basin is a north-south oriented, elongate, retro-arc foreland basin that parallels the Andean orogenic front in what is now modern day southern Chile. For >20

Myr during the Late Cretaceous, the Magallanes Basin was infilled by sediments sourced primarily from the orogenic belt (Bernhardt et al., 2012; Fildani et al., 2003; Romans et al., 2010) in a north-to-south direction, resulting in three distinctive deep-water formations (Romans et al., 2011). The Punta Barrosa Formation (Fig. 1), represents the oldest of these systems, marks the onset of coarse-grained deposition in the basin, and is characterized by dominantly unconfined turbidite lobe deposits (Fildani and Hessler, 2005; Malkowski et al., 2015).

Following the deposition of the Punta Barrosa Formation, the basin continued subsiding due to fold-thrust belt loading and the development of a deep-marine axial channel belt occurred (Romans et al., 2011). The Cerro Toro Formation represents these deposits and (Fig. 1) consists of ~2500 m of dominantly fine-grained strata with a turbiditic conglomeratic member that is interpreted as an axial (i.e., along the foredeep, parallel to the orogenic belt) channel system encased in levee deposits (Hubbard et al., 2008; Jobe et al., 2010). The coarse-grained channelized strata are ~400 m thick and are sourced from the hinterland in the north and by tributary channels coming off the Andean mountain front to the west-northwest (Crane and Lowe, 2008). To the northwest of the main study area, at Sierra del Toro (Fig. 1B), U-Pb zircon dating of three volcanic ash layers from the uppermost conglomeratic axial channel member at Sierra del Toro indicate latest Santonian to early Campanian ages (81.3 ±2.0 Ma, 81.7 ±1.7 Ma and 83.7 ±2.1 Ma) (Bernhardt et al., 2012). A volcanic ash age reported from the Cerro Toro Formation at El Chingue Bluff (82.3 ±0.3 Ma) (Daniels et al., 2016), which is ~13 km north of the study area (Fig. 1B) also indicates an early Campanian age.

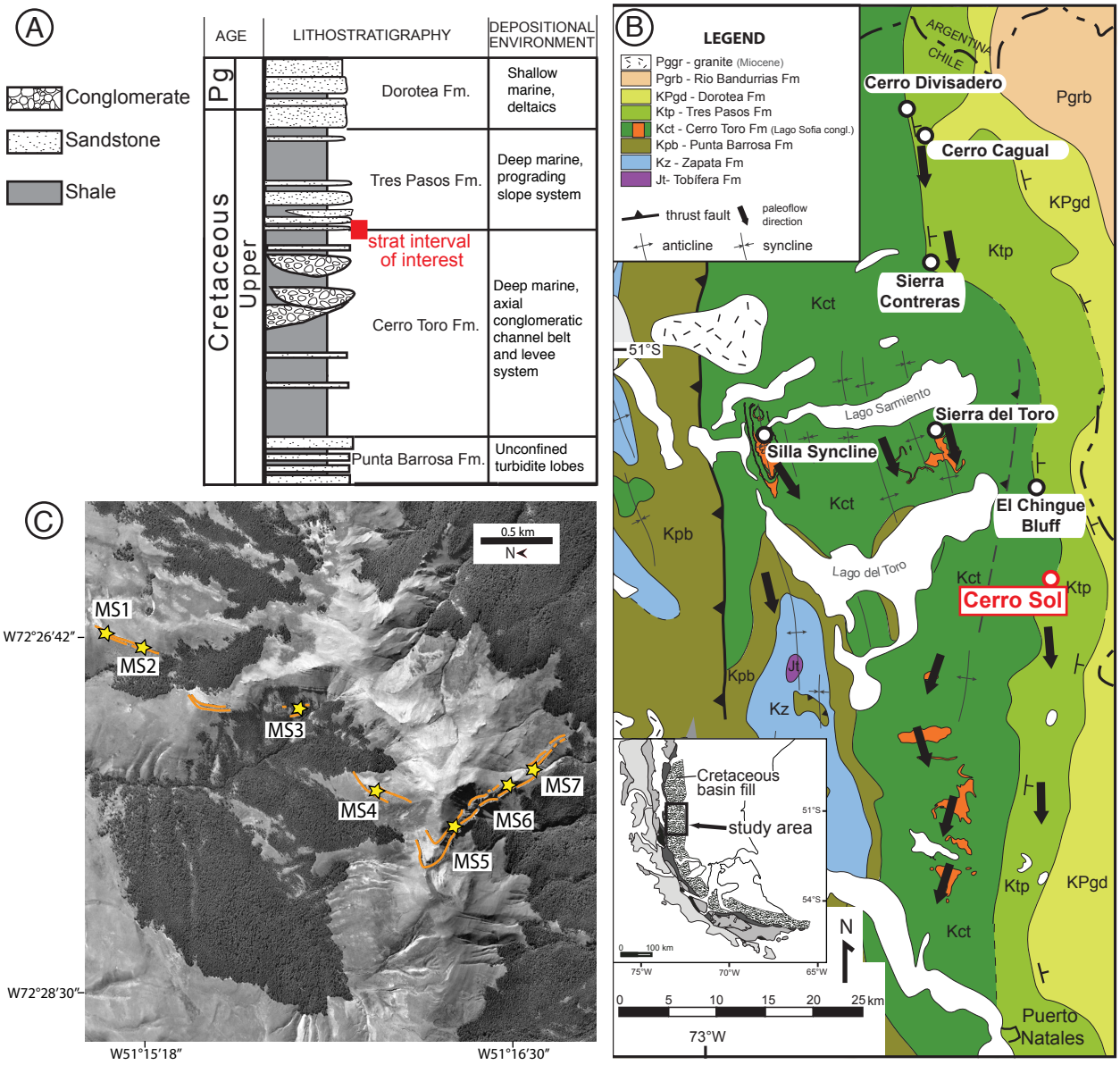

Figure 1: Geologic information and study area. A) Generalized stratigraphic column of the Magallanes Basin modified from Romans et al. 2010. Stratigraphic interval of interest is highlighted. B) Geologic map of the Magallanes Basin modified from Romans et al. 2011. Locations mentioned in the text are labeled. Study area is highlighted in red. C) Plan view of study area at Cerro Solitario. Note image has been rotated with North to the right. Orange lines are dGPS points of the outcrop around the mountain. Measured section locations are highlighted with stars.

The Tres Pasos Formation overlies the Cerro Toro Formation (Fig. 1), and represents the final stage of deep-water deposition, that consists of prograding slope systems that range from 1200 to 1500 m thick (Hubbard et al., 2010; Shultz and Hubbard, 2005; Smith, 1977). The Tres Pasos consists largely of discordant, fine-grained and concordant, fine-grained deposits encasing coarser-grained, typically sandstone with minor conglomerate deposits. The discordant fine-grained deposits are interpreted as mass transport deposits (MTDs) and the concordant fine-grained deposits as background slope and overbank deposits of the coarser-grained interpreted slope channel fills (Auchter et al., 2016; Hubbard et al., 2014, 2010; Macauley and Hubbard, 2013; Pemberton et al., 2016; Romans et al., 2009; Shultz and Hubbard, 2005).

The lithostratigraphic base of the Tres Pasos Formation is defined as the first significant sandstone encountered at the top of the Cerro Toro Formation (Katz, 1963; Smith, 1977). This contact between the fine-grained Cerro Toro Formation and coarse-grained base of the Tres Pasos Formation marks the base of what has been referred to as the Chingue Clinoform (Hubbard et al., 2010) (Fig. 2). The Chingue Clinothem is the stratigraphically oldest mapped clinothem in the Tres Pasos prograding slope system (Hubbard et al., 2010) and is equivalent to Phase 1 of Daniels et al., (2016). At El Chingue Bluff (Fig. 1B), the coarse-grained package at the base of the Chingue Clinothem was documented as an ~60 m thick, tabular, coarse-grained turbiditic package with a discordant fine-grained interval overlain by a laterally discontinuous, amalgamated coarse-grained package, which was interpreted to be a ponded intraslope mini basin controlled by large-scale growth faults (Shultz and Hubbard, 2005). This sandstone package appears to the south at Cerro Solitario where the present study is located (Fig. 1).

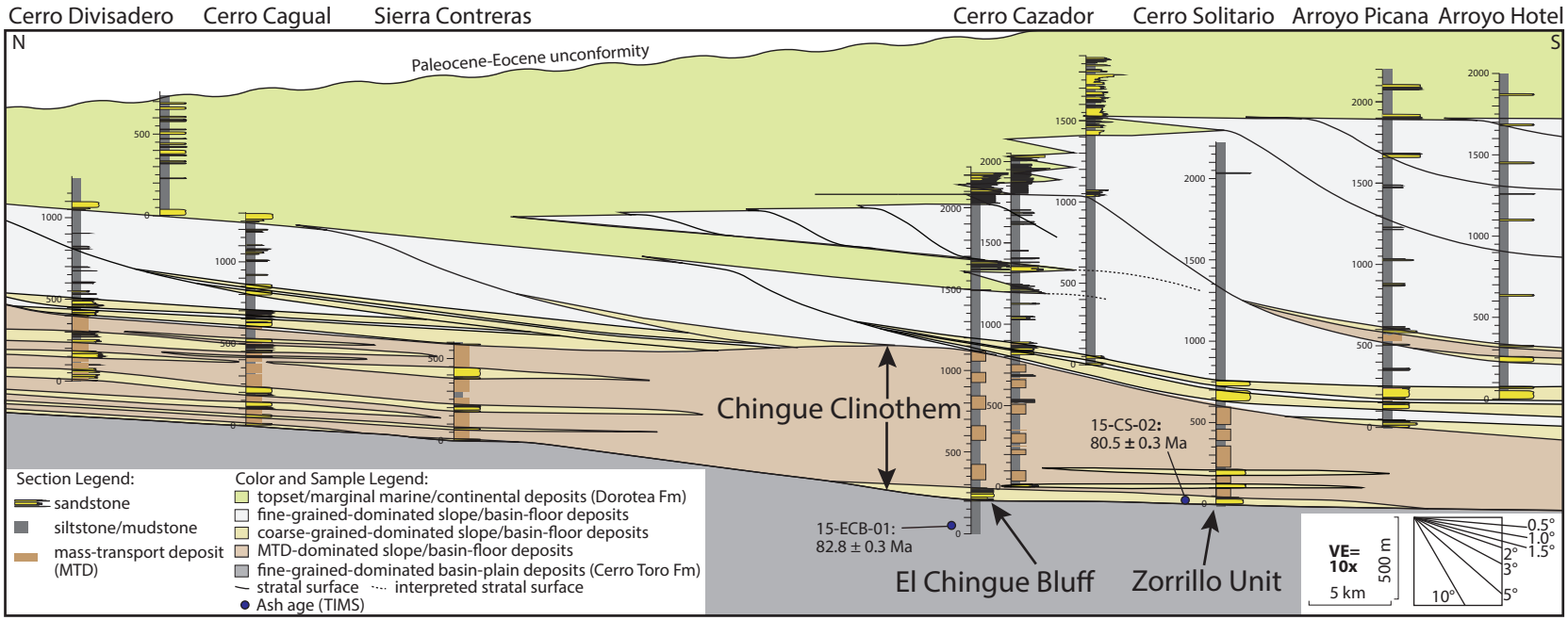

Figure 2: Regional cross section of the Magallanes Basin, modified from Daniels et al. (2016). The Zorrillo Unit and El Chingue Bluff Unit are highlighted. Ash ages are reported from Daniels et al. (2016). 15-ECB-01 is from the Cerro Toro Formation and falls within the ages reported from Bernhardt et al. (2012) for the upper Cerro Toro Formation at Sierra del Toro. 15-CS-02 is from the top of the Zorrillo Unit (see correlation diagram for location).

3. Data and Methods

The study area is a variably continuous, north to south oriented outcrop belt that provides a 3-D perspective of a turbiditic sandstone-rich unit around the top of Cerro Solitario (Fig. 1C). The thickness of this stratigraphic unit, hereafter referred to as the Zorrillo Unit, ranges from 30 to 70 m across the ~3.3 km long transect. In the southern-most part of the outcrop, continuity is exceptional; however, parts of the outcrop are exposed as steep cliffs that were inaccessible. The strata dip to the east at 15-20˚ and strike north-south, consistent with the regional structural orientation (Fosdick et al., 2011).

Eight vertical sections were logged for a total of 615 m with an average spacing of 300 m at 1:20 cm resolution using a hand lens and sand grain comparator. In addition to grain size, the presence and type of sedimentary structures, nature of bedding contacts, and any biogenic features were documented. Where paleocurrent indicators were identified, they were recorded, corrected for post-depositional tilting, and plotted on rose diagrams (*sensu* Allmendinger et al., 2011; Cardozo and Allmendinger, 2013). Paleocurrent measurements included sole marks (flutes, tool marks) and rare ripple cross lamination.

Correlations between measured sections were determined by walking out surfaces, mapping, and, in inaccessible areas, with photomosaics using a differential GPS (dGPS). The dGPS XYZ data points were double-checked in ArcGIS for accuracy and converted to a file format that was compatible with 3-D modelling software, which was used to generate surface projections to further aid correlations across covered parts of the outcrop.

Line drawings of the photomosaics capture stratigraphic architecture along with changes in bed thicknesses and faults. Where possible, line drawings were ground-truthed by measured sections, paleocurrent measurements, or other direct observation. Bed counting was done on the NW-SE transect photomosaics (Fig. 1C, MS5, MS6 and MS7) acquired by an unmanned aerial vehicle (UAV) to aid characterization of the faulted parts of the stratigraphy.

Facies associations are based on bed thickness, sandstone/mudstone ratio, degree of sandstone bed amalgamation, and sedimentary structures. Descriptive statistics were generated from the measured sections and include bed thickness, sandstone/mudstone ratio, and amalgamation ratio. These statistics are a quantitative description of the facies associations and complement the qualitative descriptions and subdivisions.

4. Facies Associations

The Zorrillo Unit is dominated by turbiditic mudstone/sandstone couplets with a high proportion of traction-dominated sandstone. Due to the number of similar bed styles, facies associations were applied to group these similar styles. The major characteristics that defined how these beds were grouped were based on sandstone bed thickness, ratio of sandstone to mudstone, and presence or absence of sedimentary structures. The term mudstone, unless specified, hereafter refers to the total fine-grained component, which includes the silt grain size.

4.1 Facies Association 1 (FA1): Mudstone interbedded with fine-grained sandstone

Facies Association 1 (FA1) consists of mudstone interbedded with very fine- to fine-grained, plane- to ripple-laminated sandstone beds that range in thickness from 2 to 25 cm (Table 1, Fig. 3A). The fine-grained intervals (mudstone and siltstone) range in thickness from 5 to 45 cm and are generally structureless, with rare vertical to sub-vertical sand-filled burrows. Sandstone beds are commonly loaded into underlying mudstone beds. The fine-grained proportion increases upwards within the sandstone beds. Small (1-5 cm) mudstone intraclasts are present in some of the sandstones. At vertical scales of several meters, the proportion of sandstone to mudstone ranges from <20% - 40%. This facies association is found stratigraphically below the Zorrillo Unit through the study interval. The contact between this facies association and the Zorrillo Unit varies through the study interval.

This facies association is interpreted as the deposits of low-density turbidity currents (*sensu* Bouma, 1962; Lowe, 1982; Talling et al., 2012). The initial deposition was through traction processes as evidenced by the lack of massive, sandy T_a division of Bouma (1962) and the occurrence of plane- and ripple-laminations in the coarse-grained part of the sedimentation unit. The increase in fine-grained (mud) proportion within the sand-dominated beds indicates a change from dominantly traction sedimentation to a mixture of traction and suspension sedimentation. The thick mudstone represents the final stages of suspension sedimentation in the waning phases of the initial turbidity current (Lowe, 1982). At the outcrop it is impossible to distinguish between the mudstone cap of the sedimentation unit and hemipelagic fallout. This facies association is

Facies Associations and Sedimentary Process Interpretation

Facies Associations	Facies	Dominant Grain Size	Sedimentary Structures	Thickness	Process Interpretations
FA1: Mudstone interbedded with fine-grained sandstone		Mudstone interbedded with very fine- to fine-grained sandstone	Mudstone: structureless; Sandstone: plane to ripple laminated, with increasing silt content	100s of meters thick (sed units: mudstone: 5-45 cm sandstone: 2-25cm)	Low density turbidity currents and hemipelagic fallout.
FA2: Thin- to medium-bedded sandstone	**F2a**	Fine- to lower coarse-grained normally grading to very fine- to fine-grained	Abundant plane and ripple laminations; Wavy to convolute laminations rare at top of beds; Missing structurless base; No amalgamation	5 to 10s of meters thick (sed units: 2-50 cm)	Low density turbidity currents, dominated by Tb-Tc.
	F2b	Upper fine- to lower coarse-grained normally grading to lower very fine- to upper fine-grained	Base of beds are occasionally structureless; When structureless base absent- laminations present throughout; Plane laminations transition upward to wavy to ripple laminations, 8-10 examples of well developed climbing ripples; Rare amalgamation	A few meters to 10s of meters thick (sed units: generally 10-50 cm, with rare examples up to 95 cm)	Low density turbidity currents, rarely overlying a high density turbidity current (Ta). Dominated by Tb-Tc.
	F2c	Upper fine- to very coarse-grained normally grading to very fine- to upper fine-grained	Structureless basal component; Abundant plane laminations common; Convolute laminations present at tops of beds; Rare climbing ripples present; Amalgamation present	Up to several meters (sed units: 20-80 cm)	High density turbidity currents, occasionally overlain by a low density turbidity current. Dominated by Ta/S3-Tc.
FA3: Thick bedded sandstone		Upper medium- to granule-rich normally grading to very fine- to fine-grained	Plane laminations and wavy to ripple laminations common in upper half of bed; Rare climbing ripples; Amalgamation common; Dewatering structures common in lower half of bed	<10 meters (sed units: 85 cm-2.35 m)	High density turbidity currents, prominent Ta/S3 overlain sometimes by low density turbidity current (Tb-Tc).
FA4: Mudstone intraclast conglomerate		Lower medium- to upper very coarse-grained grading to lower fine- to upper medium-grained	Occasionally amalgamated, high presence of mudstone intraclasts	<1 m (sed units: 15-55 cm - thickness varies laterally)	High energy deposit. Scour and bypass.
FA5: Chaotic		Dominantly siltstone with clasts from granules to sandstone wrafts	None, discordant to chaotic	Up to 10s of meters thick	Mass wasting (sliding and slumping) and cohesive-matrix supported debris flows

Table 1: Facies Associations

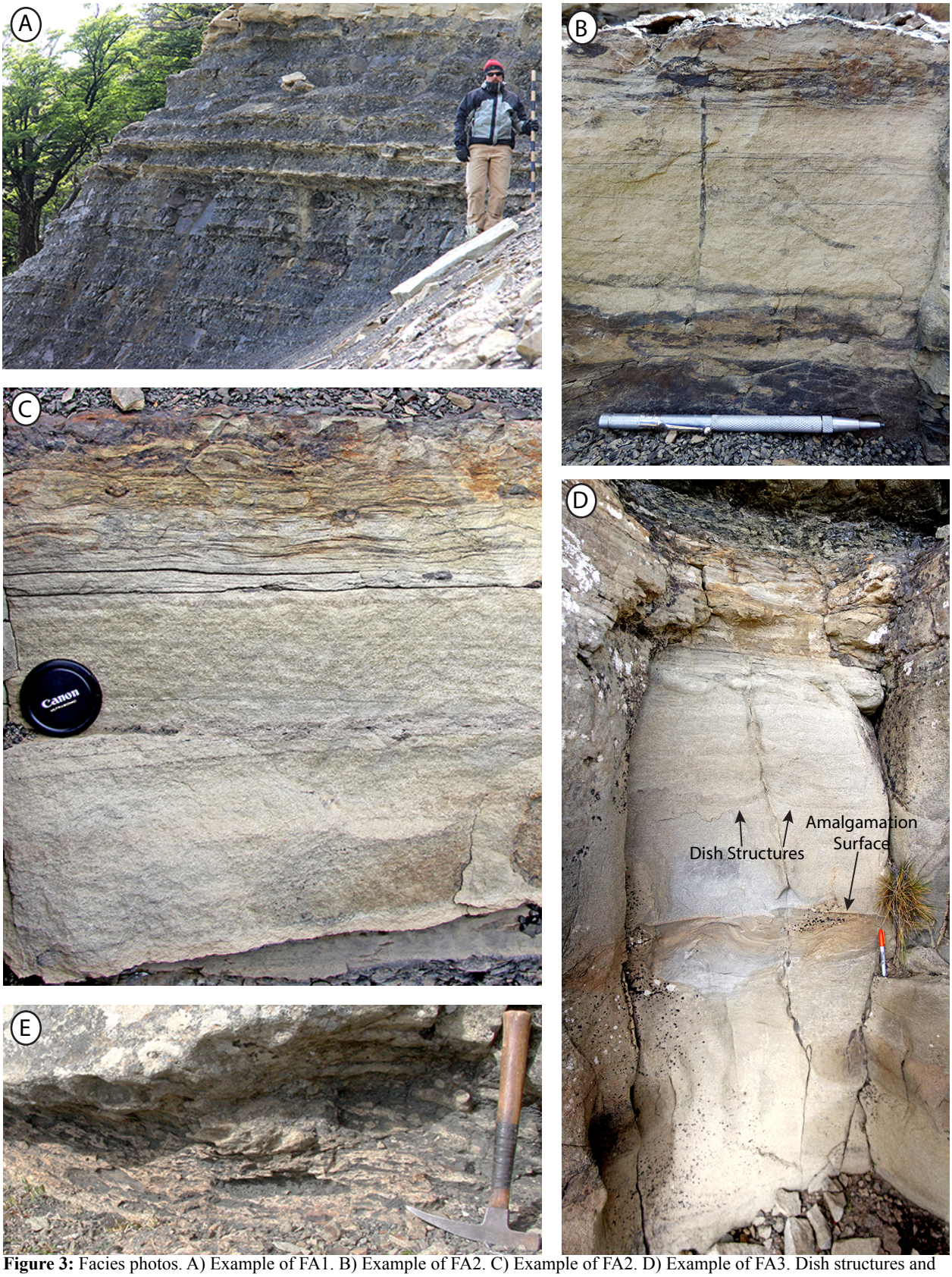

Figure 3: Facies photos. A) Example of FA1. B) Example of FA2. C) Example of FA2. D) Example of FA3. Dish structures and amalgamation surfaces common within this facies. E) Example of FA4. Note the irregular thickness and high percentage of mudclasts.

lithostratigraphically part of the underlying Cerro Toro Formation, which is interpreted as a channel-levee system (Hubbard et al., 2008; Jobe et al., 2010).

4.2 Facies Association 2 (FA2): Thin- to medium-bedded sandstone

4.2.1 Facies F2a: Thin-bedded, traction structure-dominated sandstone

Facies F2a consists of fine- to lower coarse-grained sandstone that normally grades into very fine- to fine-grained sandstone (Table 1, Fig. 3B). Sandstone beds range from 2 to 50 cm thick. Mudstone intraclast horizons with clasts <1 cm are present at the base and top of ~10% of the beds. Isolated mudstone intraclasts <10 cm in the middle parts of beds are present, but rare. Plane and ripple laminations are abundant with rare wavy to convolute laminations common near the tops of beds. The majority of beds lack a structureless basal division. Sandstone beds are overlain by a 5 to 70 cm mudstone interval that commonly has vertical to sub-vertical sand-filled burrows. Mud-filled and mud-lined burrows are present through the beds. Compared to FA1, which shares the thin-bedded characteristic, F2a is coarser grained, has a thinner mudstone cap, and includes the presence of mudclasts.

This facies association is interpreted as being deposited from low-density turbidity currents (*sensu* Bouma, 1962; Lowe, 1982; Talling et al., 2012). The initial deposition was primarily through traction processes as evidenced by the lack of massive, sandy T_a division of Bouma (1962) and the occurrence of plane and ripple laminations (Lowe, 1982). Dewatering as a result of rapid sedimentation produced the convolute laminations as the flow collapsed possibly due to a hydraulic jump (Postma et al., 2009) where the flow passes from supercritical to subcritical, usually at a break in slope. Alternatively, the

convolute laminations can be a product of sediment gravity flows interacting with the surrounding topography and shearing the top layer of the underlying bed as the upper parts of these flows are reflected by the topography (Tinterri et al., 2016). According to Tinterri et al., (2016) the intensity of the convoluted laminations is increased by the proximity to the confining topography. The distribution of this facies in relation to the inferred underlying topography makes the first option more plausible regarding the convolute laminations. An increase in intensity and occurrence of the convolute laminations within this facies is not observed. The presence of mudstone intraclasts suggest that the flow was linked to a higher energy flow updip that resulted in erosion and mudstone intraclasts being incorporated into the flow.

4.2.1 Facies F2b: Thin- to medium-bedded traction-structure dominated sandstone

Facies F2b consists of upper fine- to lower coarse-grained sandstone that grades normally into lower very fine- to upper fine-grained sandstone (Table 1, Fig. 3C). Sandstone beds range from 10 to 50 cm thick with rare examples up to 95 cm thick (Fig. 4) and amalgamation of beds is rare (Fig. 5, Fig. 6). The majority of the sandstone beds lack a structureless basal division and, instead, have laminations throughout the entire thickness of the bed. Plane laminations transition upward to wavy to ripple laminations near the top of the bed. A few bedds have well-developed climbing ripples in the upper half of the bed. Mudstone intraclast horizons with subrounded to elongate clasts ranging from <1 to 35 cm are common throughout the beds. Mud-filled and mud-lined burrows are present through the beds. Sandstone beds are overlain by a 5 to 35 cm thick mudstone interval that commonly has vertical to sub-vertical sand-filled burrows.

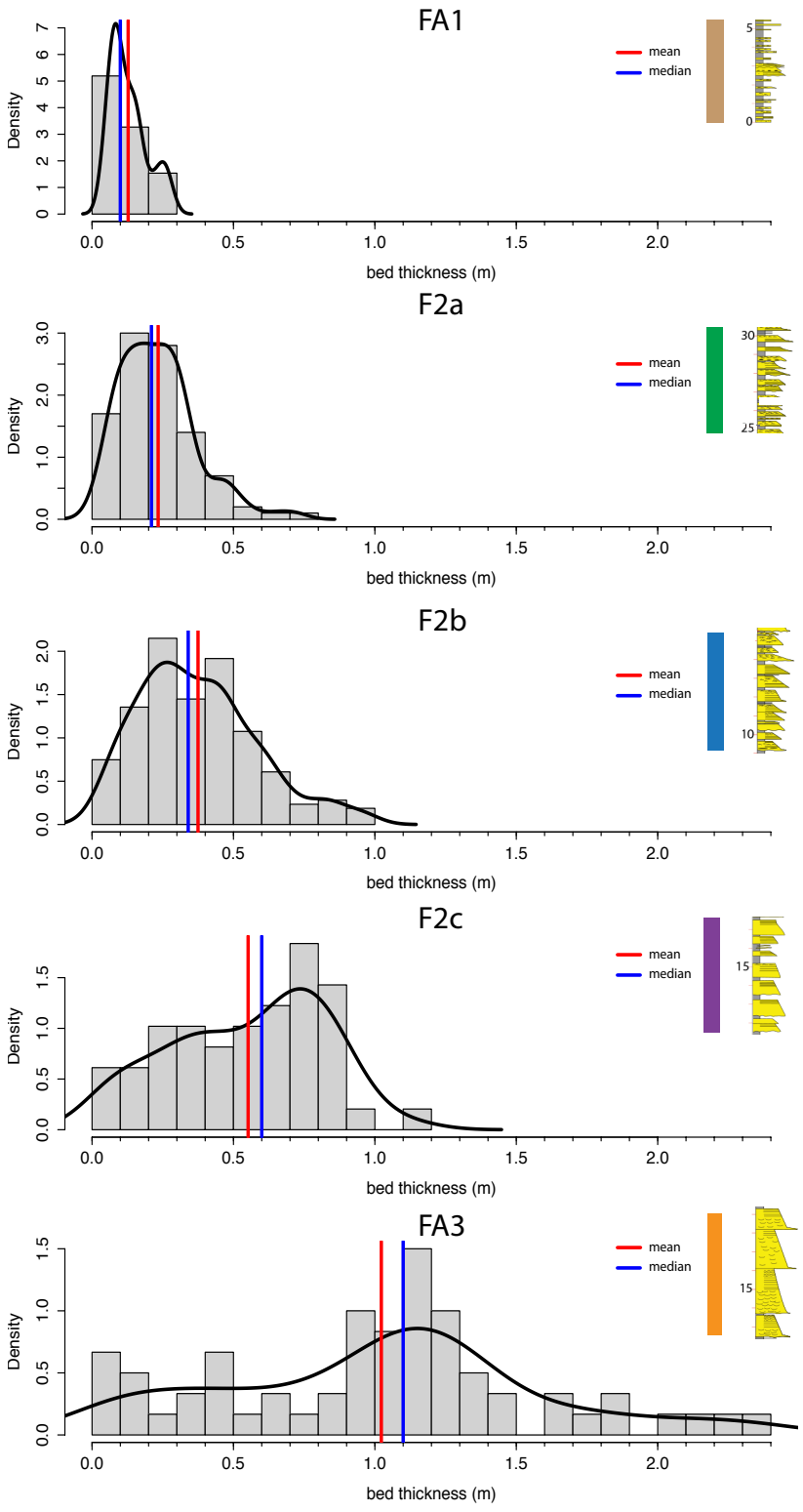

Figure 4: Summary of bed thicknesses by facies association. Density is the relative probablity that a bed will be a certian thickness. The mean and median of the bed thicknesses gradually increases with associated facies thickness. A cutoff at ~1 m is apparent. F2b has a bimodal distribution. FA3 has the greatest thickness distribution due to the method of identifying the facies associations.

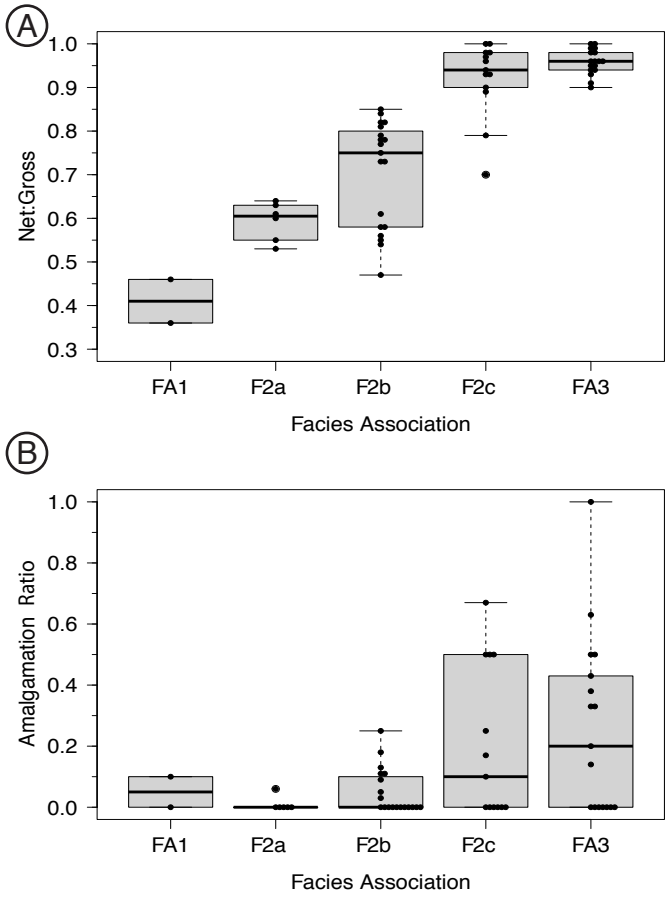

Figure 5: Summary of amalgmation ratio and net to gross by facies association. A) Facies associations plotted by net to gross. An increase in net to gross is apparent as bed thickness increases. B) Facies associations plotted by amalgamation ratio. Overall amalgamation ratio is low. An increase in amalgamation ratio is seen at bed thickness increases. Both amalgamation ratio and net to gross were calculated with continuous vertical succession. Each point represents one of those successions for that facies association.

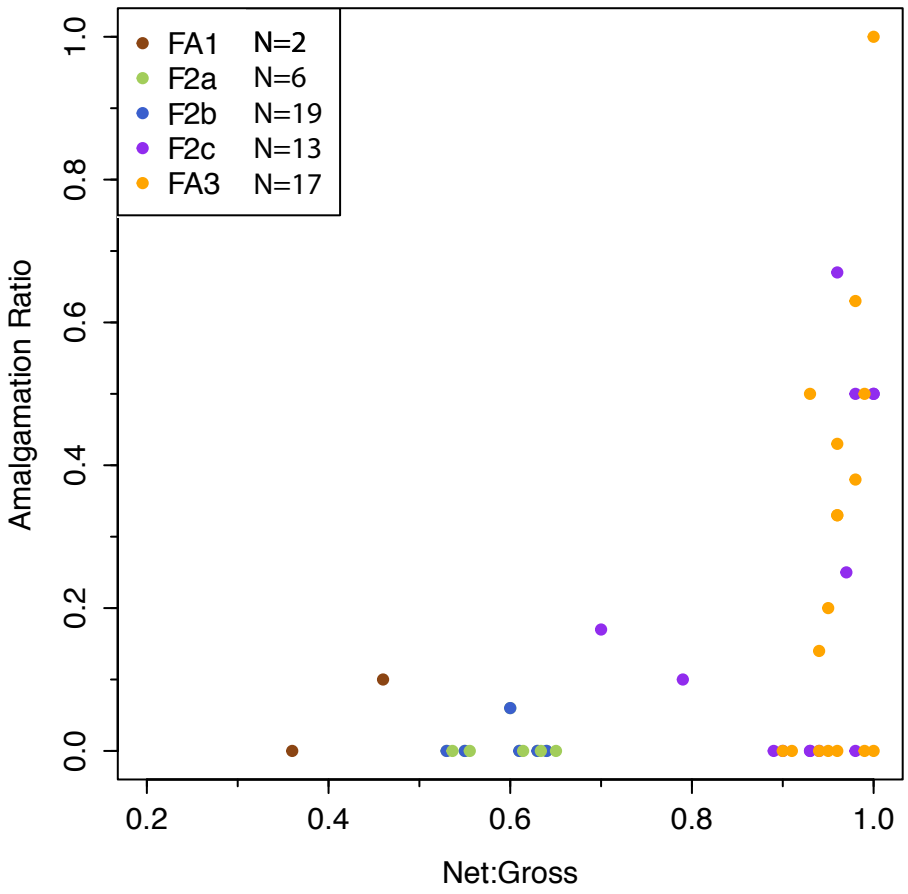

Figure 6: Crossplot of net to gross and amalgamation ratio. Low amalgamation ratio across all facies associations. Points are continuous vertical succession of facies associations. A slight increase in net to gross and amalgamation ratio is observed by facies associations.

This facies association is interpreted as being deposited by low-density turbidity currents (*sensu* Bouma, 1962; Lowe, 1982; Talling et al., 2012). The rare presence of the T_a division of Bouma (1962) and amalgamation of sandstone beds indicates that it is a slightly more erosive or a more proximal, low density current deposit than F2a. Mudstone intraclasts suggest that erosion was occurring updip and that there is potential that this low density current started out as a high-density turbidity current. The highly traction-dominated nature is evidenced by the T_b and T_c divisions of Bouma (1962) found throughout the beds. Climbing ripples are found at the top of the some of the beds in this facies association indicating that there was contemporaneous sedimentation by traction processes and suspension fallout (Allen and Leeder, 1980; Baas, 2004; Sumner et al., 2008). Climbing ripples have been found to form due to loss of confinement or a change in slope gradient (Jobe et al., 2012).

4.2.3 Facies F2c: Medium-bedded sandstone

Facies F2c consists of upper fine- to very coarse-grained sandstone that grades normally into very fine- to upper fine-grained sandstone (Table 1). Sandstone beds range from 20 to 80 cm thick and amalgamation is common with a mean and median amalgamation ratio of 0.21 and 0.10, respectively (Fig. 5, Fig. 6). When beds are non-amalgamated, a 5 to 35 cm thick mudstone interval is present overlying the sandstone divisions, commonly with sand-filled burrows. Plane laminations are abundant with ripple and wavy laminations common in the sandstone beds. Convolute lamination is also present in the top half of many of the sandstone beds with rare instances of climbing ripples. Approximately 40% of the sandstone beds have a structureless basal component.

Mudstone intraclasts horizons with subrounded to elongate clasts ranging from <1 to 35 cm are common at the base with sparse floating mudstone clasts (3 to 5 cm) found in the top half of the beds. Mud-filled and mud-lined burrows are present throughout the beds.

This facies association is interpreted to be deposits from both low- and high-density turbidity currents (*sensu* Bouma, 1962; Lowe, 1982; Talling et al., 2012) and is transitional between the thick (FA3) and thinner-bedded (F2b, F2c & FA1) facies associations. A significant number of the beds in this facies association have a basal T_a/S_3 division (Bouma, 1962; Lowe, 1982), whereas the thinner-bedded facies associations lack the basal T_a/S_3 division. The beds deposited by the low-density turbidity currents are traction dominated with T_b and T_c divisions. Where the beds have structureless basal component T_a/S_3, the T_b and T_c divisions are also present. Convolute laminations are observed near the tops of the beds that are interpreted as being deposited from a high-density turbidity current. The convolute laminations are the result of dewatering due to rapid sedimentation during flow collapse, again possibly related to a hydraulic jump (Postma et al., 2009). The observed amalgamation of the sandstone beds indicates that either the sediment gravity flows were higher in energy and eroded through the previously deposited mudstone cap or that they occurred at a higher frequency and that the fine-grained cap was never deposited. The mudstone intraclasts found at the bases of the beds in this facies association suggest that the sediment gravity flows were eroding through the fine-grained caps updip but a change in flow frequency cannot be ruled out.

4.3 Facies Association 3 (FA3) Thick bedded sandstone

Facies Association 3 (FA3) consists of upper medium- to granule-rich sandstone that normally grades into very fine- to fine-grained sandstone (Table 1, Fig. 3D). Sandstone beds range from 85 cm to 2.35 m thick and amalgamation of beds is common (Fig. 5, Fig. 6). Load structures with up to 3 cm of relief are common at bed bases. An overlying 10 to 20 cm thick, plane-laminated mudstone, commonly with vertical to sub-vertical sand-filled burrows, is present in cases where beds are not amalgamated. Dewatering structures such as dish structures and pipes are abundant in the lower half of sandstone beds whereas plane laminations and wavy to ripple laminations are common in the upper half of the beds (with rare occurrences of climbing ripples). Mudstone intraclast horizons are present in the base of some of the beds with subrounded to elongate clasts ranging from <1 to 40 cm. Mud-filled and mud-lined burrows are present sparsely throughout the beds.

The majority of the beds in this facies association are interpreted to have been deposited by sandy high-density turbidity currents (*sensu* Bouma, 1962; Lowe, 1982; Talling et al., 2012). The basal portion of these beds contain T_a/S_3 division which includes dewatering structures such as dishes and pipes, that indicate rapid sedimentation from suspension fallout (Bouma, 1962; Lowe, 1982). The upper half of the beds record traction-dominated sedimentation processes which are observed in the T_b and T_c divisions with rare climbing ripples, indicating high sedimentation rates due to sedimentation by both traction and suspension fallout processes. The sandy high-density flows were denser than the underlying substrate resulting in load structures forming.

4.4 Facies Association 4 (FA4): Mudstone intraclast conglomerate

Facies Association 4 (FA4) consists of lower medium- to upper very coarse-grained sandstone that grades into lower fine- to upper medium-grained sandstone with abundant mudstone intraclasts throughout (Table 1, Fig. 3E). Sandstone beds range from 15 to 55 cm thick. Bed thickness varies laterally due to overlying erosional truncation or lateral facies transitions into sandstone without mudstone intraclasts. Some beds have an overlying mudstone interval (5 to 10 cm thick) whereas others are amalgamated with an overlying sandstone bed. Elongate to subrounded mudstone intraclasts ranging in size from < 1 to 35 cm long are abundant and found throughout each sedimentation unit.

This facies association is interpreted to be bypass dominated and would be equivalent to Lowe's S_1 (Lowe, 1982) or Mutti's F3 (Mutti, 1992). S_1 (Lowe, 1982) results from a high-density turbidity current that creates scours and tractional features, this facies reflects bedload reworking of sediment at the base of these high-density turbidity currents. The bed thickness variations observed are the result of scouring of the sediment gravity flows as they bypassed the majority of their sediment downdip. Net bypass and erosion dominate this facies (Kane et al., 2009; Stevenson et al., 2015), which accounts for the high abundance of mudstone intraclasts throughout the sedimentation unit.

4.5 Facies Association 5 (FA5): Chaotic

Facies Association 5 (FA5) consists of discordant mudstone with discrete sandstone blocks ranging from <1 m to 10s of meters thick (Table 1). Some of the sandstone blocks within the mudstone have their internal bedding intact, whereas others are highly deformed. FA5 is dominant in the uppermost part of the stratigraphic interval studied

here (stratigraphically above the Zorrillo Unit) and rare within the sandstone-rich body. Where FA5 is present within the sandstone-rich interval, it is within the uppermost unit in 10 cm to 2 m thick beds with grain sizes up to granular within a mud-rich matrix.

FA5 is interpreted as the deposits of cohesive debris flows (*sensu* Talling et al., 2012) and chaotic, discordant mass transport deposits (Dott Jr, 1963; Martinsen, 1989; Moscardelli and Wood, 2008; Nardin, 1979). Talling et al. (2012) defined cohesive debris flows as having >20% volume cohesive (< 30 μm) mud. The high cohesive strength of the mud creates buoyancy, which can support and carry sandstone blocks significant distances down slope. Plastic fluid flow results in the movement of large contorted but relatively intact stratigraphy (Dott Jr, 1963). The mud-dominated nature allows for the movement of outsized clasts such as the sandstone blocks and granules observed.

4.6 Facies Association Statistics

Bed thickness, net to gross, and amalgamation ratio statistics were generated for facies associations FA1, FA2, and FA3 and are summarized in Table 2. These metrics are used to quantitatively describe the facies associations that were initially qualitatively interpreted above, and include bed thickness distributions, and net to gross and amalgamation ratios by facies associations and stratigraphic unit.

One of the defining factors used in identifying the facies associations was sandstone bed thickness, which is displayed by a systematic increase of the mean and median of bed thickness from FA1 to FA3 (Fig. 4). The thin-bedded facies association FA1 has a mean of 0.13 cm and a median of 0.10 cm whereas the thick-bedded facies association FA3 has a mean of 1.02 m and a median of 1.10 m. The distribution of the sandstone bed thickness

FA name	FA color	BED THICKNESS STATS				NET:GROSS AND AMALGAMATION RATIO BY FACIES						SAND/MUD RATIO PER EVENT BED
						Net:Gross (N:G)			Amalgamation Ratio (AmRat)			
		mean (m)	median (m)	stdev (m)	n =	mean	median	stdev	mean	median	stdev	%Sand
FA1		0.13	0.10	0.07	52	0.41	0.41	0.07	0.05	0.05	0.07	0.44
FA2a		0.23	0.21	0.14	100	0.59	0.61	0.05	0.01	0.00	0.02	0.61
FA2b		0.37	0.34	0.21	214	0.70	0.75	0.12	0.05	0.00	0.07	0.73
FA2c		0.55	0.60	0.27	49	0.92	0.94	0.09	0.21	0.10	0.25	0.83
FA3		1.02	1.10	0.56	60	0.96	0.96	0.03	0.26	0.20	0.29	0.91
FA4		0.34	0.35	0.15	6	n/a	n/a	n/a	n/a	n/a	n/a	n/a

Table 2: Summary of Facies Association Statistics

broadens in successively thicker-bedded facies associations because these associations are groups of beds. For example, FA3 occurrences include thick sandstone beds in close stratigraphic proximity, which commonly also include interbedded individual thin sandstone beds. FA2 has a slightly bimodal sandstone bed distribution where as FA1 and FA3 do not. There is an apparent division at approximately one meter that separates the thin- and medium-bedded facies associations FA1 and FA2 from the thicker-bedded FA3.

Net to gross (N:G or sandstone to mudstone ratio) is a measure of the total thickness of sandstone divided by the total thickness of the vertical section of interest. There is a trend of increasing N:G with increasing sandstone bed thickness (Table 2, Fig. 5, Fig. 6). Both FA2c and FA3 have relatively high N:G at over 0.9. The distributions are relatively narrow with the exception of F2b, which has two clusters of data, one around 0.6 and one around 0.75. The 0.6 cluster plots within the N:G range of F2a. FA2c includes an outlier at 0.68.

Amalgamation ratio is defined as the number of sandstone bed on sandstone bed contacts divided by the total number of sedimentation units. A sedimentation unit consists of a single flow event and includes both the basal sandstone and finer-grained capping component of mudstone (Lowe, 1982). Overall, the amalgamation ratio is low across all facies associations with the median ranging from 0.0 to 0.40 (Table 2, Fig. 5, Fig. 6). There is a slight increase in the median amalgamation ratio in FA2c and FA3, with a significant increase in the range of amalgamation ratios for those facies associations.

5. Examination of Dip Profile Transect Features

The Zorrillo Unit stratigraphically overlies fine-grained facies association FA1 (Table1), which is at least ~200 m thick in this location (and likely up to several 100s m thick) and defines the upper part of the Cerro Toro Formation (Fig. 1A). These fine-grained strata contain small growth faults (up to 30 cm of offset) (Fig. 7B, Fig. 8B) and sandstone injectites that cut across the mudstone-dominated deposits but have not been observed to cut across or terminate within the overlying Zorrillo Unit. FA5 overlies the Zorrillo Unit and contains a highly discordant and chaotic, fine-grained interval 100s of meters thick with massive contorted sandstone blocks within it (Fig. 8A). It is interpreted as a mass transport deposit that caps the succession. The Zorrillo Unit consists of facies associations FA2 and FA3.

Paleoflow indicators from within the Zorrillo Unit (n = 396) ranges from 116-195˚ with an average of 154˚ (Fig. 9, Fig. 10), which is consistent with the regional south- to southeast sediment dispersal direction documented for the Tres Pasos Formation across the Ultima Esperanza region (Hubbard et al., 2010; Romans et al., 2011). The outcrop is oriented in a north-south direction and can be subdivided into two transects that have different orientations. The northern transect is an approximately three kilometer long, semi-continuous outcrop and is NE-SW oblique to depositional-dip (Fig. 1C, MS1-MS4). The second transect is an approximately two kilometer long outcrop that offers an NW-SE oblique depositional-dip perspective (Fig. 1C, MS5-MS7). There are several characteristics of the Zorrillo Unit that change across the length of the outcrop, which represent changes from generally updip (northern most part of the outcrop) to generally downdip (southern part of the outcrop) (Fig. 9, Fig. 10). The stratigraphic framework in

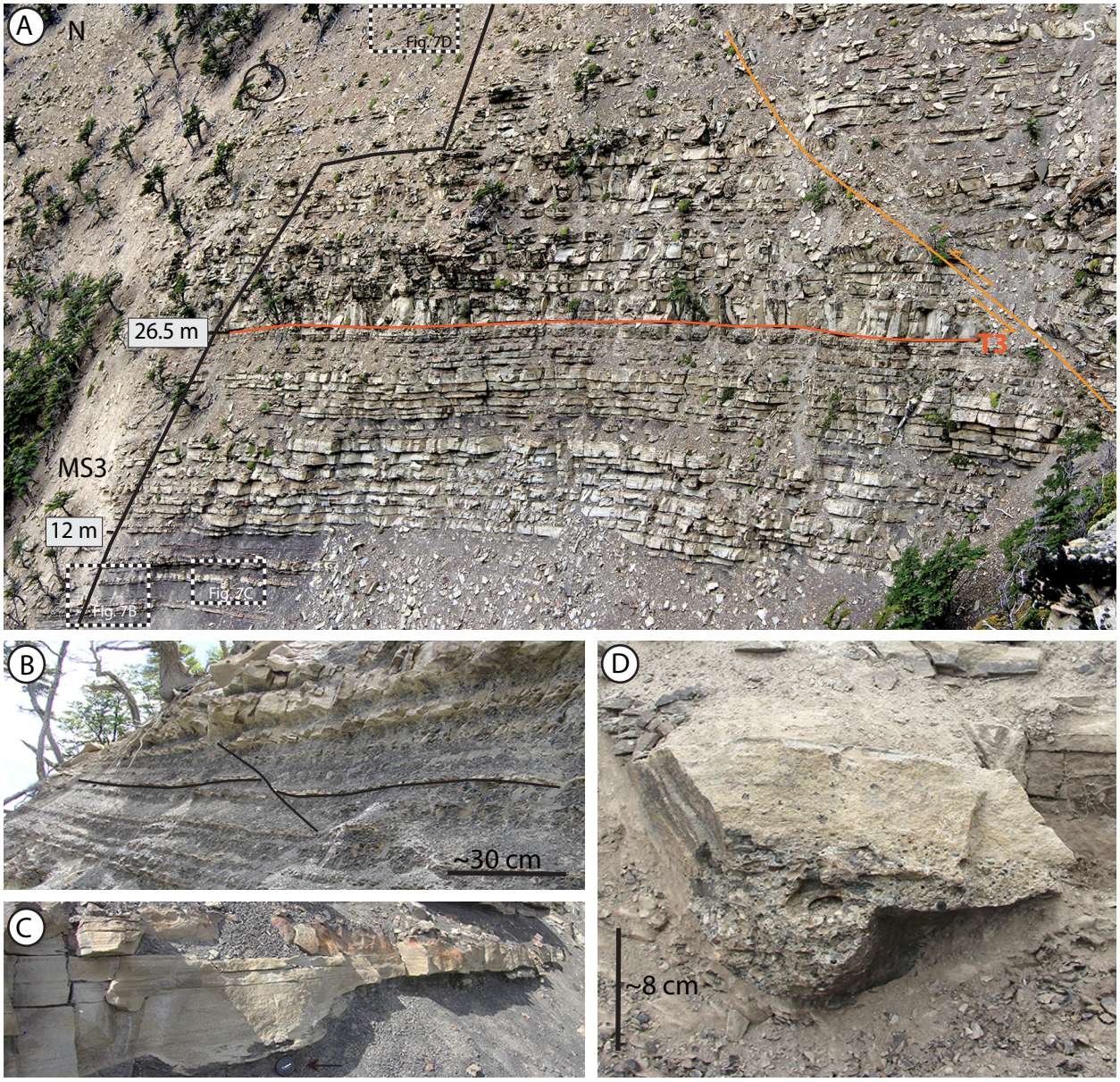

Figure 7: Photos from the central outcrop at MS3, highlighting several features. A) photo of entire outcrop. MS3 is highlighted in black with corresponding meterages. T3 surface from correlation diagram is noted with the red line. Orange line is a reverse fault interpreted to be from Oligocene-Miocene tectonism associated with uplift of these units. Locations of photos B, C, and D are highlighted in the call out boxes. Geologist circled for scale. B) Small-scale growth fault with ~15 cm of offset. C) Example of bed scour in the lower unit. Note lens cap for scale. D) Scour filled with a pebble lag (largest grains 5-6 mm) at the top of the succession.

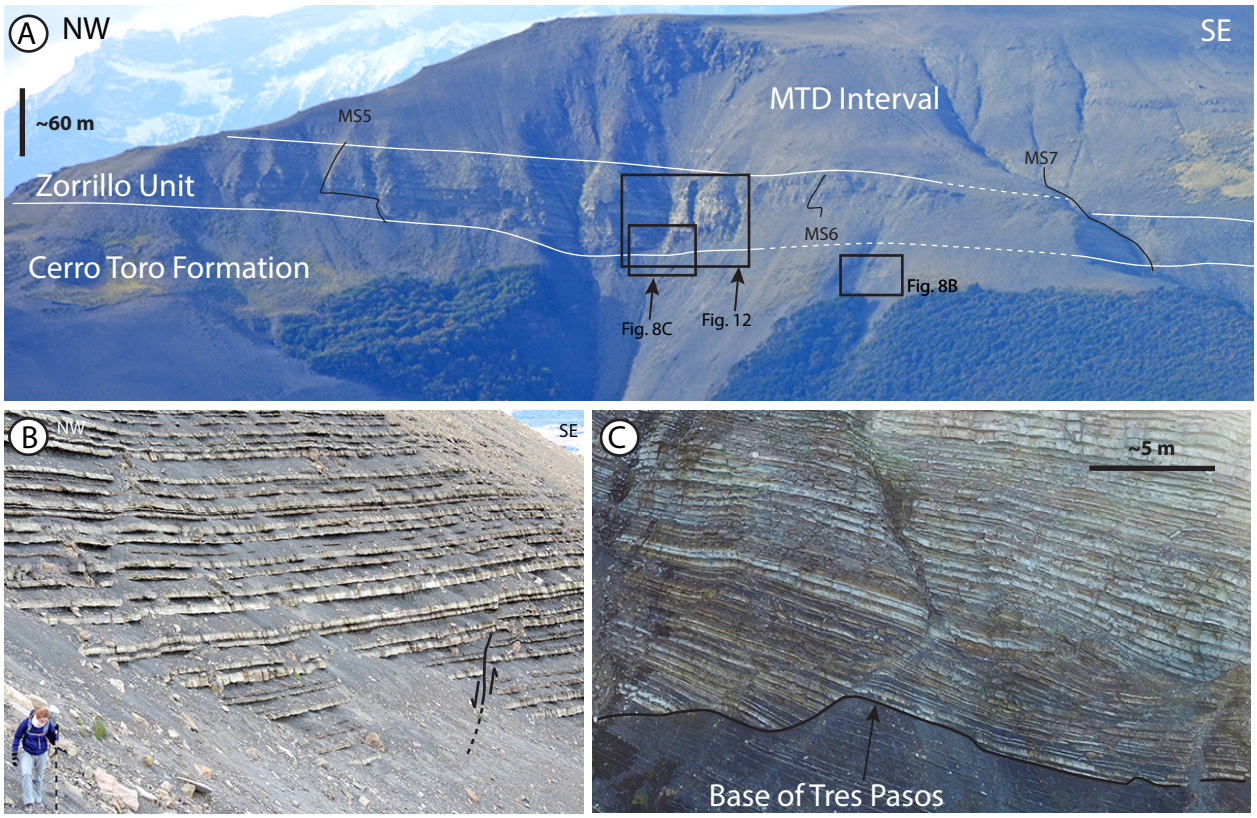

Figure 8: Overview of southern transect. A) Photomosaic of the entire southern transect with MS5, MS6 and MS7 locations highlighted in black. Black boxes show locations Figures 8C, 8B and 12. White lines denote the mapped boundaries of the Zorrillo Unit. B) Small growth fault in underlying strata. C) Photo highlights the highly irregular contact between the Zorrillo Unit and the underlying strata.

Figure 9: Correlation diagram. Measured sections are oriented in a North to South line. See Fig. 1B for section locations. Three phases discussed in the text are highlighted. Marker beds 2 and 3 correlate to marker beds on Fig. 12. The T surfaces are based on mapped and inferred correlations and make up the unit bounderies. T3 is the first correlation line that traverses the entire outcrop. Notice the thickness changes that occur below it. The correlation diagram is hung on the MTD surface at the top and bounded by the Cerro Toro Formation on the bottom. The location of the ash sample discussed in the text is shown.

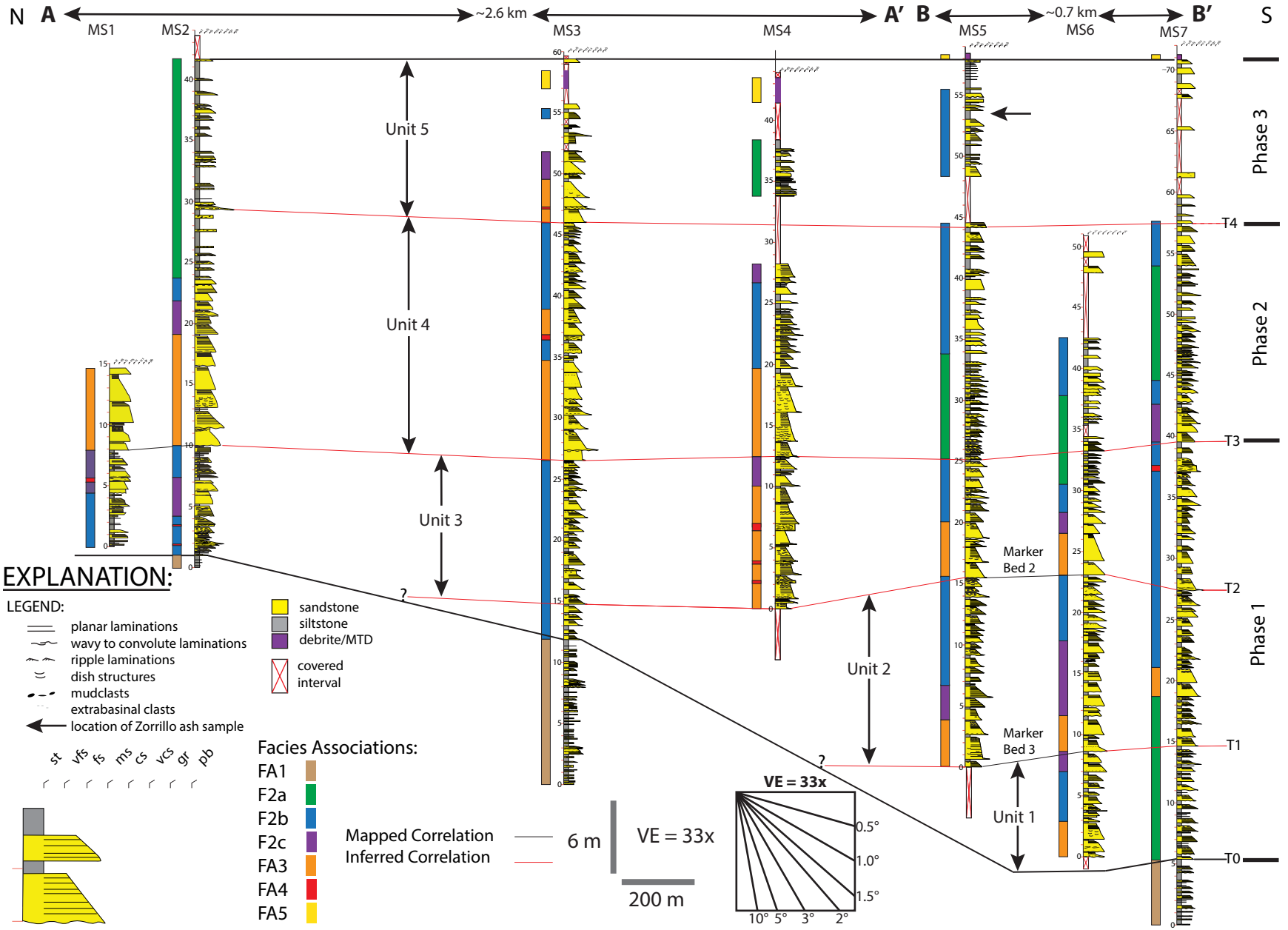
N
A
~2.6 km
A′
B
~0.7 km
B′
S
MS1
MS2
MS3
MS4
MS5
MS6
MS7
Unit 5
Unit 4
Unit 3
Unit 2
Unit 1
Marker Bed 2
Marker Bed 3
Phase 3
Phase 2
Phase 1
T4
T3
T2
T1
T0
EXPLANATION:
LEGEND:
planar laminations
wavy to convolute laminations
ripple laminations
dish structures
mudclasts
extrabasinal clasts
location of Zorrillo ash sample
st
vfs
fs
ms
cs
vcs
gr
pb
sandstone
siltstone
debrite/MTD
covered interval
Facies Associations:
FA1
F2a
F2b
F2c
FA3
FA4
FA5
Mapped Correlation
Inferred Correlation
6 m
VE = 33x
200 m
VE = 33x
0.5°
1.0°
1.5°
10°
5°
3°
2°

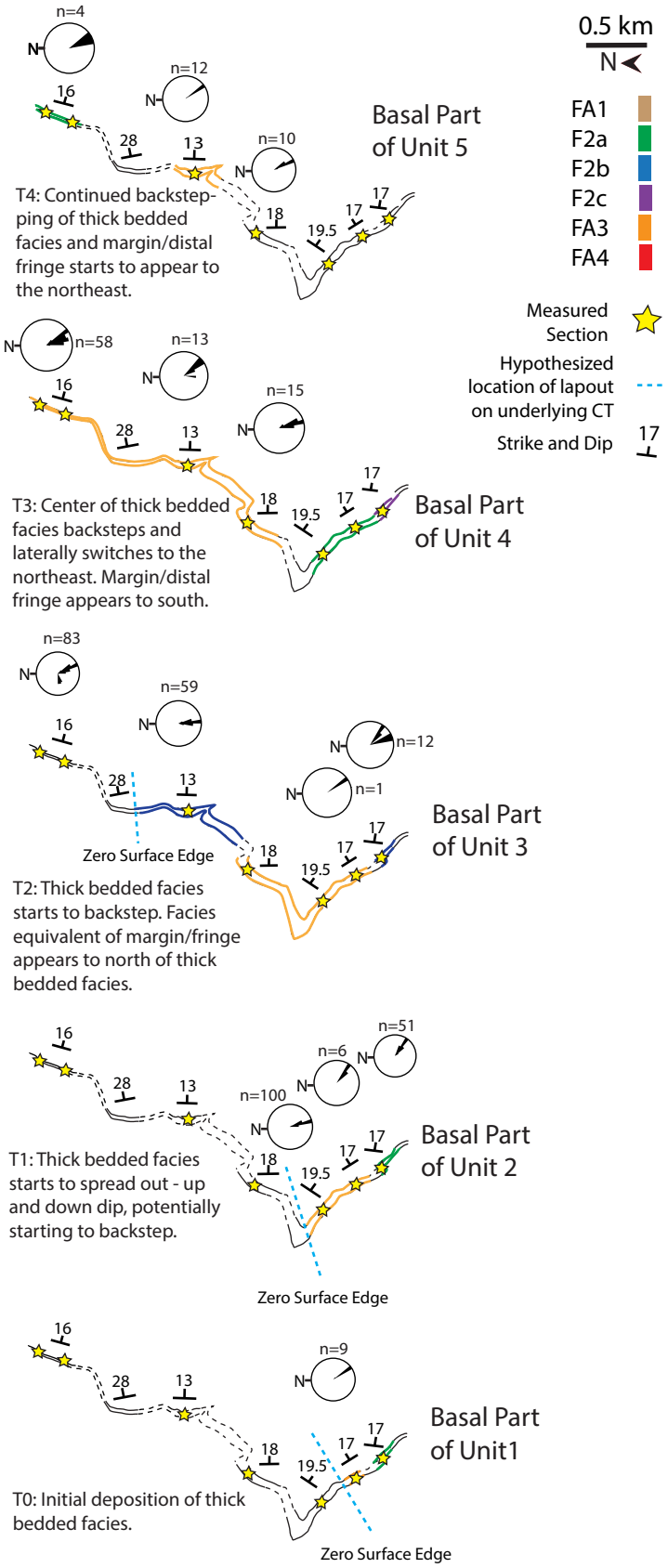

Figure 10: Planform stratigraphic evolution of the Zorrillo Unit. North is to the left. T1, T2 and T3 show a backstepping of FA3. T4 shows a backstepping as well as spreading out. T5 is limited due to lack of data. Outline of outcrop is from dGPS point. Facies associations highlighted are from the basal part of the Unit. Paleoflow diagrams have been rotated so that North is to the left. Paleoflow diagrams consist of sole marks. Blue dotted line in T1, T2, and T3 represent the hypothesized lapout surface on to the underlying Cerro Toro Formation. CT is short for Cerro Toro Formation.

which these changes occur consists of 5 units separated by surfaces (T0-T4). These surfaces are identified by internal correlations. There are two types of correlations: mapped and inferred. The mapped correlations are based off of photomosaics and walking out surfaces. The inferred correlations were made based on how the measured sections fit within the bounding surfaces of the lower Cerro Toro Formation and the overlying mass-transport deposit. Within this framework, the inferred correlations were based on facies association relationships. When lateral changes in facies associations did not correlate, changes in bed scale relationships within the facies association guided the interpretation. The characteristics to be discussed below include: (1) nature of the basal contact with underlying strata, (2) overall stratigraphic thickness, (3) stratigraphic and spatial distribution of evidence for erosion and bypass, and (4) occurrence and style of normal faults.

5.1 Contact with underlying Cerro Toro Formation

The contact between the underlying Cerro Toro Formation (FA1) and the Zorrillo Unit is variably expressed, from an abrupt transition in the northern (updip) sections (Fig. 11A, Fig. 11C) to gradational with a localized highly irregular contact in the southern (downdip) part of the outcrop (Fig. 12A). In the north, there is a sharp boundary between the dark-colored underlying mudstone and the overlying lighter-colored sandstone beds. The underlying strata consist of mudstone with millimeter-thick siltstone beds. Downdip ~0.6 km at MS3 (Fig. 7) the contact is much more diffuse. The dark mudstone dominates the lower part of this transition, but thin (~10-20 cm), light-colored sandstone beds are more common than the mudstone beds. The sandstone beds increase in number and

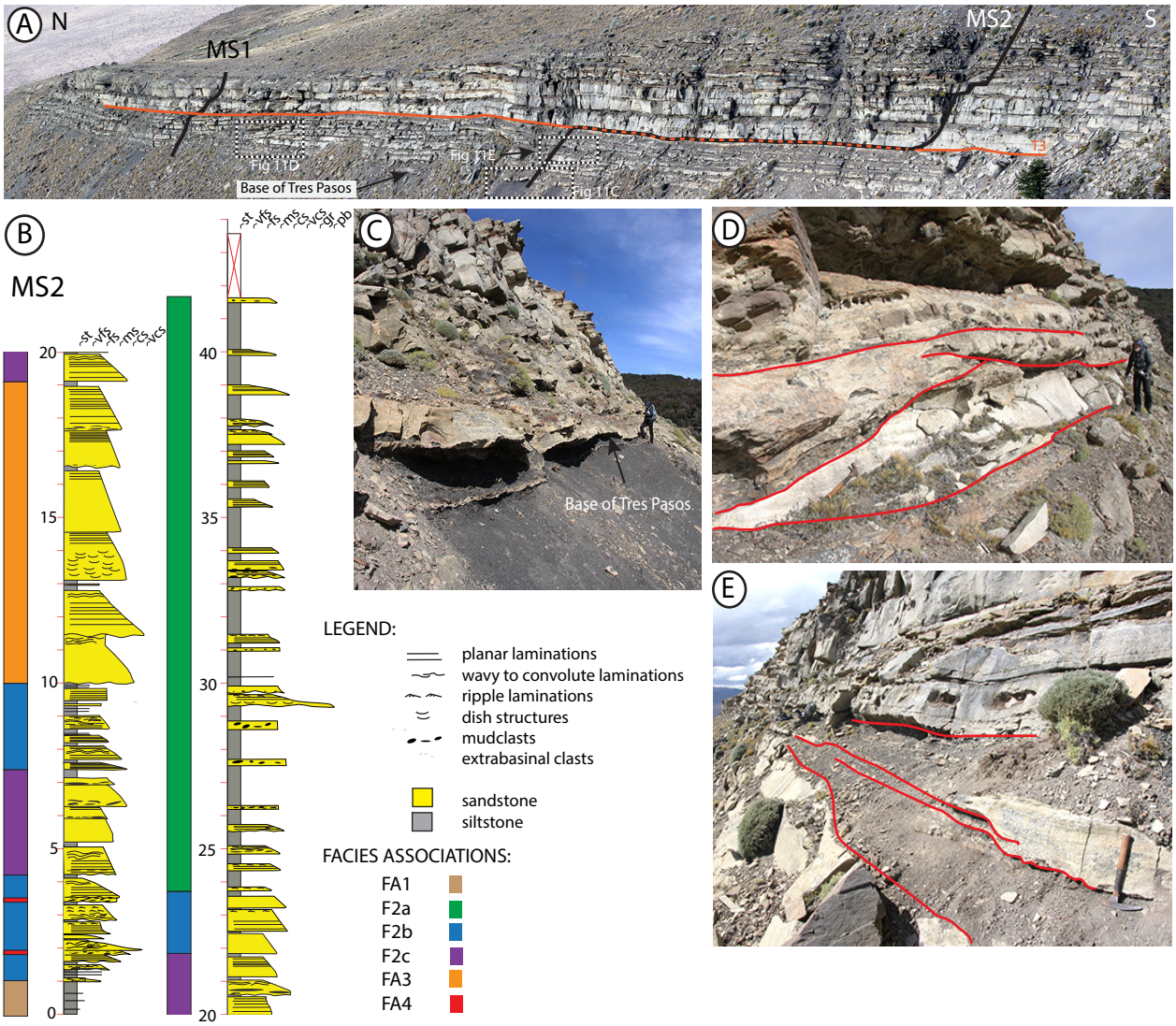

Figure 11: Overview of north outcrop. A) Photo mosaic of north outcrop. MS1 and MS2 are highlighted with black line. Note the thickening of the outcrop to the south. Black and white boxes are insets shown in C, D and E. T3 surface is highlighted in orange. B) Complete measured section of MS2 with legend and facies associations. C) Contact between the Tres Pasos Formation and Cerro Toro Formation. D and E) Red lines show scouring of beds that is common in the lower half of the updip part of the outcrop belt.

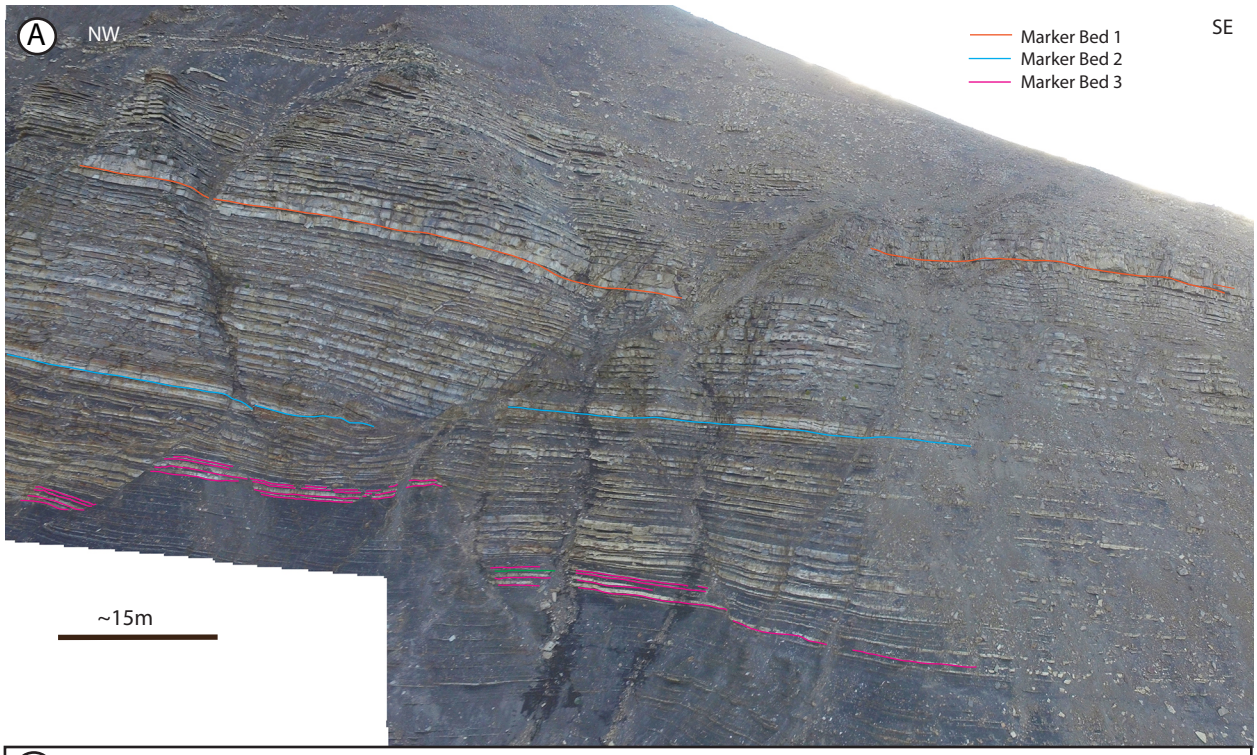

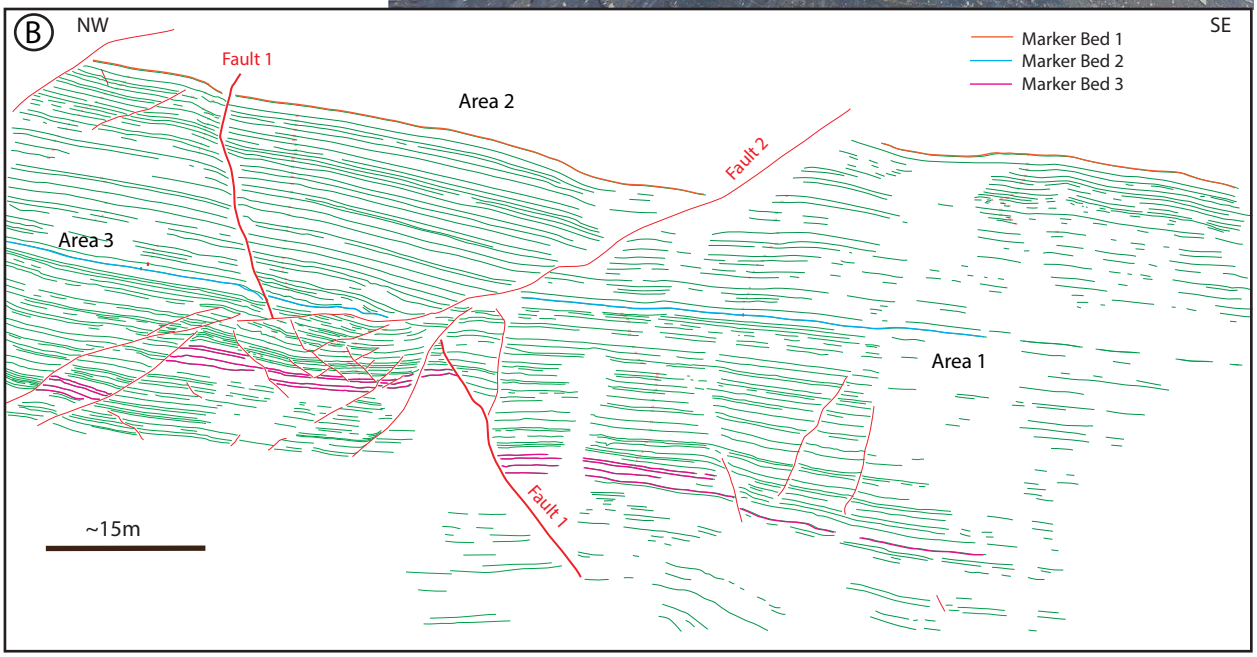

C

	Photo 1			Photo 2			Photo 3			
Area	1	2	3	2	3	4	2	3	4	5
Top half	37	34	32/33	34	35	34	31	33	34	34
Bottom half	31	n/a	n/a	n/a	37	29	n/a	33	34	17
Total:	68				72	63		66	68	51

Figure 12: Southern Transect Faults. A) Uninterpreted photo mosaic of part of the face of the southern outcrop. Marker beds highlighted correspond to marker beds in B. B) Line drawing of photo mosaic in A. Green lines are bases of coarse-grained packages. Red lines are interpreted to be faults. Photo was broken up into discrete areas between faults. Area 1,2, and 3 are pictured in this photo. C) Results of bed counting exercise. Multiple photo mosaics were used and 5 discrete areas were identified. The marker beds broke each area into an upper and lower half. Where a complete section was not able to be counted, N/A was recorded.

thickness up section, whereas the mudstone and siltstone beds become thinner and less common, and significantly thicker (~40-50 cm) sandstone beds cap this transition. Downdip, at the southern outcrop transect (Fig. 8C, Fig. 12A), this contact is gradational compared to what is observed in the central outcrop. However, within the southern outcrop transect there is a localized area that deviates from this trend and exhibits a highly irregular contact between the Cerro Toro Formation and the overlying Tres Pasos Formation. This irregular surface is the result of the normal faults that cut through the sandstone body (discussed in section 5.4).

5.2 Stratigraphic Thickness

The thickness of the Zorrillo Unit from the basal contact (T0 on Fig. 9) to the base of the overlying MTD (the datum on Fig. 9) increases across the ~3.3 km long outcrop transect by ~75 %. In the updip part of the outcrop, at MS1 and MS2, the entire unit measures ~40 m in thickness and is ~50 m in thickness ~0.7 km downdip at MS3. The most distal part of the outcrop at MS5, MS6, and MS7, which is ~0.75 km downdip from MS3, the entire unit is at its maximum observable thickness of ~70 m (Fig. 9).

The T3 surface is the lower-most marker that can be traced across the outcrop in its entirety; T1 and T2 are not continuous across the transect. Below this marker, the stratigraphic thickness of the Zorrillo Unit increases downdip, whereas no stratigraphic thickness changes are seen above this marker across the outcrop when the stratigraphy is preserved (Fig. 9). In the updip part of the outcrop, there is ~10 m of stratigraphy below the T3 marker, which in the downdip area of the outcrop increases to ~35 m. The

stratigraphically lowest units, Units 1 and 2, which are present only in the downdip section are interpreted to lap out updip against the underlying Cerro Toro Formation.

5.3 Stratigraphic and Spatial Distribution of Evidence for Erosion and Bypass

Another group of characteristics that change across the transect are shallow erosional scour surfaces, lag deposits and facies association FA4 (mudstone intraclast conglomerate, Fig. 3E). In the most updip part of the outcrop, the beds below the T3 marker exhibit erosional surfaces (Fig. 11D, Fig. 11E). These erosional surfaces include beds that have been cut into resulting in erosional relief up to 2 m across 5-10 m laterally, which are observed to wedge or pinch out (Fig. 11D, Fig. 11E). Approximately 10-20% of the beds below the T3 marker in the most updip part of outcrop have a thick mudstone intraclast lag at the base of the sandstone bed versus <10% of sandstone beds seen downdip. The beds with the thick mudstone intraclast lags contain up to very coarse sand in grain size. Approximately 20 m above the T3 marker at MS1 and MS2, similar features are observed such as beds being cut into and are expressed as beds pinching out with extrabasinal pebbles up to 2 cm in size mantling the erosional surfaces.

Downdip at MS3, there are significantly fewer beds below T4 that exhibit erosional features. Only one bed is documented to have a significantly cut into the underlying substrate with relief of ~50 cm (Fig. 7C). Sandstone beds below the T3 marker with mudstone intraclasts at their base are rare, though there are several beds with thin mudstone intraclast horizons. No erosional scours were observed in Unit 4. Within Unit 5 (Fig. 9) there is a notable scour filled with an extrabasinal pebble lag with grain sizes up to 5-6 mm. It cuts down into the underlying mudstone bed resulting in ~12 cm of

erosional relief (Fig 7D). Above the T3 marker, FA4 is observed only once in Unit 4 and once in Unit 5 with rare instances of mudstone intraclast lags at the base of sandstone beds in both units.

At the farthest downdip part of the outcrop, at MS5, MS6, and MS7, evidence for erosion that is noted updip are absent throughout the stratigraphy. No scours, no beds pinching or wedging out, and no significant lag deposits were observed in downdip positions. Basal mudstone intraclast lags are observed in the sandstone beds but they are relatively fewer than what is observed updip.

The evidence for erosive flows suggests that the flows were entraining the substrate and it was subsequently being bypass downdip. These erosive features are interpreted as indicating bypass and have been documented by Stevenson et al., (2014) for deepwater systems. The interpreted bypass occurring at Cerro Solitario is small scale compared to overall Magallanes deepwater system. Regionally, the sediment that was bypassed at Cerro Solitario was not a significant amount, nor did it travel vary far compared to the overall system. Evidence for bypass is more common updip and significantly less common in downdip areas relative to the number of beds in that stratigraphic section.

5.4 Normal faults

Normal faults are observed across the outcrop and vary in configuration. As noted above, growth faults are present in the strata of the Cerro Toro Formation underlying the Zorillo Unit across the outcrop transect (Fig. 7B, Fig. 8B). A reverse fault cutting the Zorrillo Unit near MS3 was observed (Fig. 7A); however, reverse faults in the study area are interpreted to be from Oligocene-Miocene tectonism associated with uplift of the

succession (Fosdick et al., 2011) and is not discussed further. Normal faults are the most common fault documented within the Zorrillo Unit and have been identified in the southern transect that run northwest to southeast and no normal faults have been identified in the updip areas near MS1, MS2, and MS3.

The normal faults present in the downdip sections produce a highly irregular contact with the underlying Cerro Toro Formation (Fig 8C, Fig. 12). Bed counting and line drawings were done to help understand the timing of these faults. The stratigraphic thickness and number of sandstone beds does not change across the faults (Fig 12), suggesting that these normal faults are not related to growth faulting, and are post depositional. While they are interpreted to be post-depositional, it is uncertain how much later after deposition the faulting occurred. Due to the nature of the faults it is thought that the faulting is not related to the Oligocene-Miocene tectonism (Fosdick et al., 2011) and more likely compaction-related structures related to the emplacement of the overlying MTDs. This makes the timing of these post-depositional faults occurred after the deposition of the sandstone body but still within the timeframe of the construction of the overlying prograding slope system.

5.5 Stratigraphic Evolution and Evidence for Containment

The stratigraphic evolution of the Zorrillo Unit is expressed differently both spatially and vertically throughout the outcrop (Fig. 9, Fig. 10). In the updip area (at MS1 and MS2), the lower third of the section is dominated by erosional features, with the common occurrence of scours and mudstone intraclast conglomerates. Above the T3 marker at this location, which separates Units 3 and 4, the appearance of thick-bedded FA3 indicates a

transition to dominantly depositional processes. This is expressed as upward bed thinning, which could be indicative of compensational stacking (Prélat and Hodgson, 2013; Spychala et al., 2015). The base of Unit 5 (the T4 surface) at this updip location indicates renewed erosional processes with a pebble lag filled scour. There are significantly less erosional features below the T3 marker downdip (MS4) in Units 1, 2, and, 3, but the same vertical pattern is observed; i.e., bypass in Units 2 and 3, deposition in Unit 4, and bypass again in Unit 5. However, depositional processes dominate the entire succession in the southernmost transect at MS5, MS6 and MS7 through all stratigraphic units. The upward bed-thinning motif is repeated several times above and below the T3 marker in Units 4 and 5 before being capped by the overlying MTD.

Laterally, Units 1 and 2 are interpreted to onlap the underlying Cerro Toro Formation and, thus, are not present in updip positions. Where they are present, Units 1 and 2 consist of the upward bed-thinning motif, which suggests that the depocenter is undergoing compensational stacking as the axis of the depocenter moves to account for the filling up of the accommodation. Unit 3 transitions from erosional and bypass dominated to exhibiting depositional features downdip. Upward bed-thinning motif is common through Unit 4 across the outcrop indicating it is dominated by depositional processes. Unit 5 is marked by erosional scours and lag deposits in the updip area. A lack of data makes it difficult to definitively conclude if bypass indicators such as large scours and cuts into underlying strata are present downdip in Unit 5 or if it is similar to the lower units and transitions laterally from bypass processes to depositional processes. The overall history can be summarized into three phases. The first phase is one of bypass and non-deposition in areas of relatively high topography and deposition in areas of relatively

lower topography (Units 1-3). The second phase consists of widespread deposition across the entire transect (Unit 4). The third and final phase records an increase in the occurrence of erosion and bypass (Unit 5) (Fig. 9).

Containment of the Zorrillo Unit at Cerro Solitario is interpreted by the following criteria. An irregular, lower surface has been documented based on mapping of the Zorrillo Unit. Units 1 and 2 are inferred to onlap onto the underlying fine-grained deposits of the Cerro Toro Formation, which suggests that there was topography at the time of deposition. As a result of this irregular surface, the entire unit thickens in a downdip direction away from the interpreted topographic high. Evidence for the mechanism that created the irregular topography is lacking due to outcrop exposure, but it is hypothesized that it is the result of offset created by a large-scale growth fault as small-scale growth faults (<1 m of offset) have been documented in the underlying fine-grained strata (Fig. 7B, Fig. 8B) (see section 6.2 for discussion on growth faulting). The documented spatial distribution of erosion supports the containment interpretation. With the exception of the updip part of Unit 3, the majority of the units record depositional processes that correspond to deposition in topographic lows. The erosional featuers seen in the updip section of Unit 3 could be explained by the sediment gravity flows entering the accommodation as they reached a new base level within the available accommodation.

The low level of amalgamation (Table 2, Fig. 5, Fig. 6) throughout the Zorrillo Unit is suggestive of containment. Sandstone mudstone couplets with thick mudstone caps were one of the diagnostic characteristics that Pickering and Hiscott (1985) noted about contained deposits. While mudstone caps are present, they lack the classic meters thick

mud caps indicative for the complete ponding of the incoming sediment gravity flows. The preservation of mud caps at Cerro Solitario suggests that while complete containment was not achieved, partial containment of the incoming flows was achieved. With low topographic relief, flows would be able to overtop the surrounding topography and flow stripping would occur and the finer upper portion of the sediment gravity flow would not be contained by the surrounding topography and would bypass down slope.

The majority of climbing ripples are in facies association F2b at the tops of Units 1 and 2, at the southern end of the outcrop, which suggests that the depositing turbidity currents were experiencing a decrease in flow related to a change in slope gradient and/or the turbidity currents were expanding as a result of a decrease in confinement (Jobe et al., 2012). The decrease in slope gradient or the loss of confinement could be related to the filling of the accommodation, which is interpreted to have been controlled by growth fault movement. The process of expanding flows due to the loss of confinement is the author's preferred interpretation due to the fact that the climbing ripples appear at the tops of Unit 1 and 2. Deposition of Unit 1 due to the low relief, filled up and healed the seafloor topography. As flows expand across the healed topography they formed climbing ripples. When the growth fault moved again and created accommodation, flows were captured again and the process was repeated to the top of Unit 2. This scenario is proposed with the assumption that the growth faulting at Cerro Solitario occurred in discrete steps. Alternatively, the climbing ripples formed as a result of the flows coming down a paleoslope and slowing down as they reached the base of that slope. These observations correspond to the occurrences of first phase of bypass and non-deposition in

areas of relatively high topography and deposition in areas of relatively lower topography.

Convolute laminations result from rapid sedimentation. The majority of the convolute laminations found in FA2 of Units 1, 2, and 3 (Fig 9), which supports the idea that the turbidity currents were feeling the bounding surface causing flow decelerations and reflections and resulting in rapid sedimentation (Tinterri et al., 2016). Again these convolute laminations are found in the first phase described above, and are related to deposition in topographic lows and bypass across topographic highs.

Ripple measurements (n=25 from two locations) indicate east-northeast paleoflow, which is a deviation from the regional paleoflow of south-southeast. In contained basins, the upper parts of the sedimentation units can record the complex interaction between the flow and the topography, which is reflected in sedimentary structures that indicate flow paths that deviate from the regional paleoflow (Kneller et al., 1991). Flow reversal occurs when a flow feels the effects of a topographic high on the seafloor and is redirected (Haughton, 1994; Kneller et al., 1991; Pickering and Hiscott, 1985).

6. Discussion

6.1 Cerro Solitario and the Fill-and-Spill Model

Full containment of sediment gravity flows is possible and depends on the flow size relative to the accommodation. The interplay between flow size and available accommodation leads to a spectrum of flow deposits that results from the flow being completely contained to experiencing no containment from the bounding surfaces. The ‘fill-and-spill’ model of Prather et al. (1998) identified, using seismic-reflection and well

log data, fully contained sediment gravity flow deposit within the salt-withdrawal mini-basins of the Gulf of Mexico. Sinclair and Tomasso (2002) applied Prather et al.'s (1998) fill-and-spill model to the Tertiary Alpine basins and integrated outcrop and subsurface data to create a model of infilling for contained turbidite basins. The Sinclair and Tomasso (2002) model is characterized by four phases: 1) flow ponding, where the incoming sediment gravity flows are completely trapped, 2) flow stripping, where the upper finer-grained and more dilute portion of the flows escapes over the confining topography, 3) flow bypass, which can be expressed as either incision into the filled basin and topographic high at the spill point thus providing a conduit to a lower base level or as abandonment as feeder channels do not incised into the topographic high at the spill point and instead search for a new route to a lower base level, and finally 4) blanketing of the basin resulting in backfilling of the conduit that transported the sediment in phase 3, which raises the local base level leading to renewed sediment accumulation. This reduction in gradient from the backfilling can allow for the development of meandering channel systems across the top of the basin. This is documented in both Gulf of Mexico examples (Prather et al., 1998) and in the Annot Sandstone (Sinclair and Tomasso, 2002). In the Sinclair and Tomasso (2002) model, phases 1 and 2 represent infill in the proximal subbasin. The flow stripping that occurs in the proximal basin in phase 2 is represented as a potential fine-grained sediment drape in the distal basin with an upward bed-thickening sequence, the result of more coarse grains overcoming the bounding margin. Phase 3 and 4 can be expressed in both the proximal and distal sub basins.

While Zorrillo Unit at Cerro Solitario has features that indicate some degree of flow containment it lacks the evidence for complete flow ponding seen in phase 1 of the

proximal Tertiary Alpine sub basins, where 2-3 m thick, structureless mudstones occur and the sandstone-to-mudstone ratios of these deposits range from 40-50% (Sinclair and Tomasso, 2002). Within the Zorrillo Unit at Cerro Solitario, mudstone thicknesses are at most 50 cm with an average sandstone-to-mudstone ratio per unit of 70% (Table 3). Prather et al. (2012) suggested that lower relief perched aprons in the Gulf of Mexico would result in higher net-to-gross values. This sandstone-to-mudstone ratio of 70% for Cerro Solitario is on the low end of that observed for the phase 2 of the Tertiary Alpine sub basins, which ranges from 70-95% (Sinclair and Tomasso, 2002) and suggests that at the time of deposition relief could have been significantly less.

Both the Gulf of Mexico seismic-reflection examples and the Tertiary Alpine Basin outcrop succession are significantly thicker systems than the Zorrillo Unit at Cerro Solitario. The Gulf of Mexico mini basin is ~3.25-3.5 sec (two way travel time), or approximately 250-500 m thick (Prather et al., 1998) and the thickness of the Tertiary Alpine Basins are on the order of 100s of meters to kilometers (Sinclair and Tomasso, 2002), whereas the Zorrillo Unit at Cerro Solitario is 40-60 m thick (Fig. 9). This thickness discrepancy, in part, can be explained by the lack of topographic relief observed at Cerro Solitario. Partially contained turbidites lack the earliest stage of flow ponding and subsequently capture the entire flow. If the entire flow is not captured, part of it will be deposited in adjacent and/or in down-slope regions. For Cerro Solitario, this lack of relief is due to the interpreted mode of confinement, growth faulting. In the Gulf of Mexico, confinement is the result of salt tectonics (Prather et al., 1998) and in the Tertiary Alpine Basins confinement is interpreted to be the result of faulting related to mountain building deformation (Sinclair and Cowie, 2003). Both modes of confinement

North	NET TO GROSS BY STRATIGRAPHIC UNIT						South
	MS1	MS2	MS3	MS4	MS5	MS6	MS7
Unit 5		0.46	0.9	0.66	0.53		
Unit 4	0.97	0.68	0.86	0.79	0.6	0.55	0.64
Unit 3	0.73	0.82	0.76	0.82	0.82	0.69	0.73
Unit 2			0.7			0.77	0.74
Unit 1						0.79	0.57

Table 3: Net to gross ratios by stratigraphic unit across the transect.

resulted in the creation of relief large enough to fully capture the incoming sediment gravity flows. At Cerro Solitario the interpreted confinement related to growth faulting produced significantly less relief that could not contain the flows completely, and allowed for a significant amount of sediment to be bypassed down dip.

The lack of full containment of the sediment gravity flows at Cerro Solitario, makes the application of the fully contained depositional model not straightforward and, potentially, not applicable (Table 4). The record of infilling is clearly more complex at Cerro Solitario than the simplified end-member model discussed above. A fully contained unit is missing from the lower succession and there are phases of flow stripping present. Individually, Units 1 and 2 can be considered consistent with the flow-stripping phase of Sinclair and Tomasso (2002), especially with regards to their mudstone to sandstone ratios. Both Units 1 and 2 show cycles of increasing flow stripping; at the bases of Units 1 and 2, the thick-bedded facies (FA3) is present with decreasing sandstone bed thickness upwards through the section implying that a greater portion of the flow had been stripped away as the accommodation had been filled and healed by the earlier FA3 flows. Considering the distribution of FA3 within Unit 3, it appears to be located spatially in a different position from FA3 within Unit 1 and 2. Unit 3 shows a small backstepping of FA3, which could be the result of compensational stacking, which occurred due to growth faulting. If the growth fault moves differentially, there is the potential for the available accommodation to be altered by the growth faulting and as a result, lateral switching and/or backstepping of the depocenter could occur. Alternatively, this could be the result of the healing of topography by the deposition of Units 1 and 2 and the backstepping of Unit 3 caused by the fact that as the sediment deposition by gravity flows

Fill-and-Spill Model (Prather et al., 1998)		Outcrop based Fill-and-Spill (Sinclair & Tomasso, 2002)	Partially Contained Outcrop Model (This Study)	Partially Contained Outcrop (Shultz & Hubbard, 2005)	Partially Contained Salt Withdrawl Mini-Basin (Yeilding & Apps, 1994)
Ponded Assemblage	Ponding Fill Bypass Slope Readjustment Backfill Drape	Flow Ponding Flow Stripping	Bypass in proximal; Flow Stripping in distal Backstepping and Blacketing	Flow Stripping Blanketing	Multiple Repeated Variations of: Fill Bypass
Bypass Assemblage	Ponding Slope Progradation Slope Retrogradation Drape Mass Wasting	Bypass Backfilling	Renewed Bypass	Bypass	Drape

Table 4: Comparisons between Fully Contained and Partially Contained Systems.

was now smaller than the available accommodation. Units 1, 2, and 3 are equivalent to Phase 1 identified earlier (Fig 9, Fig. 10). Unit 4 shows a significant backstepping and blanketing of the FA3 facies. This healed topography (Phase 2) allows for renewed scours in Unit 5, which suggests a relative increase in flow bypass during this time even though fully channelized deposits did not develop (Phase 3). The Zorrillo Unit shares some aspects of the classic fill-and-spill model such as early flow stripping phases and later phases of flow bypass and flow blanketing, but displays some clear differences from this model. The initial ponding stage does not occur and Units 3, 4, and 5 do not follow the later stages of flow bypass followed by flow blanketing of the fill-and-spill model. Units 3, 4, and 5 also exhibit depositional backstepping and blanketing followed by flow bypass. The complexity of the partially contained deposits was a product of low relief and how these relief changed in response to the growth faulting.

6.2 Comparison of Cerro Solitario to El Chingue Bluff

Approximately 13 km to the north of Cerro Solitario at El Chingue Bluff (ECB) (Fig. 1B) is a spectacular exposure interpreted to be correlative to the Zorrillo Unit documented here. The ECB exposure is an ~2 km long dip profile transect that displays paleoflow to the south-southeast. The stratigraphic succession documented at ECB consists of: 1) fine-grained strata of the Cerro Toro Formation; 2) a thick-bedded sandstone package ~30 m thick that shows upward thickening and coarsening cycles; 3) a laterally discontinuous, chaotic interval and coarse-grained sandstones that contains mudstone rich intraclasts ~1-3 m thick capped by; 4) a coarse-grained amalgamated sandstone (Shultz and Hubbard, 2005). The turbiditic sandstone package studied at ECB

was interpreted to be a product of prograding distributary channels, followed by debris flows and channel lag deposits and capped by a channelized turbidity current deposit (Shultz and Hubbard, 2005).

This vertical succession has several important differences from what is documented at Cerro Solitario. For example, in the updip location at Cerro Solitario, the stratigraphic expression displays bypass, deposition, and then renewed bypass before the system undergoes major switch to MTD-dominated deposition. In the downdip area of Cerro Solitario, the stratigraphic expression reflects dominantly depositional processes throughout the section; no channelized features are observed across the top of the downdip part of the Zorrillo Unit.

The sandstone unit at ECB was interpreted by Schultz and Hubbard (2005) as an intraslope, ponded, growth-fault-controlled, mini basin. The basis for this interpretation is a documented growth fault with ~50 m of maximum offset. Evidence for this depositional model includes unambiguous stratal thickening and thinning across the fault, sandstone beds within the down-thrown block that lap out against the fault, and the presence of at least one other large-scale growth fault with ~50 m offset in the underlying stratigraphy (Shultz and Hubbard, 2005). Building off of the fill-and-spill model; the idea of linked depocenters could be applied to both ECB and Cerro Solitario. There are instances of channels cutting across the tops of contained deposits and indicate bypass of the deposit as the system searches for the new base level (Adeogba et al., 2005; Jobe et al., 2016; Prather et al., 2012). The interpreted channel at the top of the ECB succession potentially could have been a conduit to bypass sediment across the top of the sandstone package and farther down slope to Cerro Solitario.

6.3 Implications for Slope System Initiation in the Magallanes Basin

The Zorrillo Unit at Cerro Solitario marks the transition between two very different deepwater depositional systems: the underlying conglomeratic axial channel-levee system of the Cerro Toro Formation (Hubbard et al., 2008; Jobe et al., 2010) and the overlying prograding slope system of the Tres Pasos Formation (Hubbard et al., 2010; Romans et al., 2009; Shultz et al., 2005). A recent compilation of new and published U-Pb zircon ages from volcanic ashes and detrital samples, including a volcanic ash age from within the Zorrillo Unit at Cerro Solitario with an age of 80.5 ±0.3 Ma (Daniels et al., 2016), confirms the stratigraphic relationship of the Zorrillo Unit to the two different deepwater depositional systems.

There are several hypotheses regarding the sources of the coarse-grained sediment that makes up the Zorrillo Unit at Cerro Solitario and at ECB. One is these sandstone bodies represent overbank deposition from the underlying conglomerate Cerro Toro axial channel belt. For a conglomeratic channel system, it is not unrealistic to have overbank deposits of medium to coarse-grained sand (Hickson and Lowe, 2002; Mansfield, 1979). The location of Cerro Solitario and ECB is ~5 km to the east of the axial channel belt, which would place them on the flanks of the levee that was building up adjacent to the channel. Ash ages from Cerro Solitario and ECB (Daniels et al., 2016) place the timing of deposition of the units at Cerro Solitario and ECB within the age ranges reported from the uppermost units of the Cerro Toro axial channel belt (Bernhardt et al., 2012). Paleoflow in an overbank setting would be expected to be dispersive. At both Cerro Solitario and ECB it matches regional paleoflow, which makes this hypothesis less

favorable. Another hypothesis is that the sediment entered the basin from a transverse (tributary) feeder channel system to the west. In the underlying Cerro Toro, a tributary channel has been documented at the Silla Syncline in the north (Fig. 1B), which indicates a relative proximity to the slope of the emergent fold-thrust belt. If there was a tributary channel, it is no longer preserved. A third hypothesis is that these sandstone bodies are the distal equivalent to coeval Tres Pasos stratigraphy to the north (Fig 1B, Fig. 2). However, outcrop characterization in the northern part of the Magallanes Basin from Cerro Divisadero (Romans et al., 2009) to Cerro Cagual (Auchter et al., 2016) to Sierra Contreras (Armitage et al., 2009), which is >40 km north of the outcrop at Cerro Solitario and was originally thought to be the updip equivalent to the units at Cerro Solitario and ECB (Shultz et al., 2005), indicate that these units show a different style of deposition and are younger than the units at Cerro Solitario and ECB (Daniels et al., 2016).

Therefore the preferred hypothesis is that the sandstone bodies along the Chingue Clinothem are not related to the overlying prograding slope system of the Tres Pasos Formation but are related to the shut off of the point source that was feeding the underlying axial channel belt of the Cerro Toro Formation. Building on previous workers Romans et al., (2011), suggested that the axial Cerro Toro channel had a canyon point source updip, however no evidence for a preserved canyon has been found updip. I hypothesize that there was an allogenic control, either sea-level rise and/or subsidence of the hinterlands that resulted in the switch from a system fed by a point source to a delta-fed system. The underlying Cerro Toro axial channel-levee system at Sierra del Toro (Jobe et al., 2010) and Cordillera Manuel Señoret (Hubbard et al., 2008) is positioned ~5 km westward from the Cerro Solitario and ECB outcrops. Assuming that the basin axis

did not shift, Cerro Solitario and ECB could represent off-axis deposits. As the allogenic controls were felt through the system, coarse-grained sediment started to build up on the shelf and eventually stopped making it to the distal parts of the basin. Alternatively, as the updip canyon started to collapse, basin scale MTDs could have rerouted sediment to the east as it blocked off the axis of the basin. Either way, the collapse of the feeder canyon would have started to choke off the sediment routing system that was supplying sediment to the distal part of the basin. Subsequently the last sediments to make it through the remnants of the old system were caught within the depocenters found at Cerro Solitario and ECB.

The transition from an axial conglomeratic channel system to a prograding slope system potentially happened within the 2-3 millions of years, between the age of the Cerro Toro channel belt (Bernhardt et al., 2012) and age of Zorrillo Unit at Solitario (Daniels et al., 2016). The sandstone bodies at ECB and Cerro Solitario therefore record the shut off, showing that while coarse-grained material still made it down the canyon system, it occurred at a significantly reduced amount. The evidence that Cerro Solitario and ECB are linked in the fill and spill fashion indicates that the deep-marine slope system was still out of grade (*sensu* Pyles et al., 2011; Ross et al., 1994) and in the process of reaching equilibrium. During the following reorganization of the system, the canyon walls likely failed resulting in the massive MTDs capping the succession at Cerro Solitario.

7. Conclusion

The Zorrillo Unit at Cerro Solitario of the Late Cretaceous Magallanes Basin represents a transition the underlying deep-water Cerro Toro conglomeratic axial channel belt and the overlying Tres Pasos prograding deep-water slope system. Mapping of the variably continuous Zorrillo Unit across a 3.3 km long transect on Cerro Solitario allowed identification of facies associations and correlation of stratigraphic units within the 40-70 m thick turbiditic sandstone package. The Zorrillo Unit is interpreted to be partially contained based on the following criteria: differences in stratigraphic thickness across the outcrop, the observation of a modified fill-and-spill motif, spatial changes in units (bypass in north and deposition in south), presence and thickness of mudstone thickness, irregular underlying topography, sedimentary structures, and flow reversals. The succession observed in the Zorrillo Unit does not follow the general stratigraphic succession that is identified in widely applied fill-and-spill models. The observations and data from the Zorrillo Unit suggeset instead a model for partial flow containment. Two periods of flow stripping occurred as a result of changing relief related to growth fault movement. Backstepping and then blanketing of the accommodation area followed as the topography was healed. Bypass occurred in the final depositional stage. The major control on stratigraphic evolution was the amount of available relief. While deposits of partially contained depocenters share many of the same characteristics in outcrop as fully contained depocenters these deposits contain several distinctive differences. Therefore the application of standard fill and spill model does not work for partially contained depocenters; thus, I present a new conceptual model based on the interpretation of partial confinement is present here. Building off of the idea of linked sub-basins helps to provide

insight into the greater Magallanes Basin. The Zorrillo Unit represents the final stages of sedimentation from the Cerro Toro axial channel belt before the system ultimately switched off.

References

Adeogba, A.A., McHargue, T.R., Graham, S.A., 2005. Transient fan architecture and depositional controls from near-surface 3-D seismic data, Niger Delta continental slope. AAPG Bulletin 89, 627–643. doi:10.1306/11200404025

Allen, J.R.L., Leeder, M.R., 1980. Criteria for the instability of upper-stage plane beds. Sedimentology 27, 209–217.

Allmendinger, R.W., Cardozo, N., Fisher, D.M., 2011. Structural geology algorithms: vectors and tensors. Cambridge University Press.

Amy, L.A., Kneller, B.C., McCAFFREY, W.D., 2007. Facies architecture of the Gres de Peira Cava, SE France: landward stacking patterns in ponded turbiditic basins. Journal of the Geological Society 164, 143–162.

Armitage, D.A., Romans, B.W., Covault, J.A., Graham, S.A., 2009. The Influence of Mass-Transport-Deposit Surface Topography on the Evolution of Turbidite Architecture: The Sierra Contreras, Tres Pasos Formation (Cretaceous), Southern Chile. Journal of Sedimentary Research 79, 287–301. doi:10.2110/jsr.2009.035

Auchter, N.C., Romans, B.W., Hubbard, S.M., 2016. Influence of deposit architecture on intrastratal deformation, slope deposits of the Tres Pasos Formation, Chile. Sedimentary Geology 341, 13–26. doi:10.1016/j.sedgeo.2016.05.005

Baas, J.H., 2004. Conditions for formation of massive turbiditic sandstones by primary depositional processes. Sedimentary Geology 166, 293–310. doi:10.1016/j.sedgeo.2004.01.011

Bernhardt, A., Jobe, Z.R., Grove, M., Lowe, D.R., 2012. Palaeogeography and diachronous infill of an ancient deep-marine foreland basin, Upper Cretaceous

Cerro Toro Formation, Magallanes Basin. Basin Research 24, 269–294. doi:10.1111/j.1365-2117.2011.00528.x

Bersezio, R., Felletti, F., Micucci, L., 2005. Statistical analysis of stratal patterns and facies changes at the terminations of “turbiditic” sandstone bodies: the Oligocene Cengio Unit (Tertiary Piedmont Basin). GeoActa 4, 83–104.

Bouma, A.H., 1962. Sedimentology of some flysch deposits: a graphical approach to facies interpretation. Elsevier Pub. Co.

Cardozo, N., Allmendinger, R.W., 2013. Spherical projections with OSXStereonet. Computers & Geosciences 51, 193–205. doi:10.1016/j.cageo.2012.07.021

Crane, W.H., Lowe, D.R., 2008. Architecture and evolution of the Paine channel complex, Cerro Toro Formation (Upper Cretaceous), Silla Syncline, Magallanes Basin, Chile: Architecture and evolution of the Paine channel complex. Sedimentology 55, 979–1009. doi:10.1111/j.1365-3091.2007.00933.x

Daniels, B.G., Auchter, N.C., Matthews, W., Hubbard, S.M., Romans, B.W., Stright, L., 2016. The Evolution of Deepwater Slope Systems on Retroarc Foreland Basin Margins: Insights from Detrial Zircon Geochronology, Tres Pasos Formation, Magallanes Basin, Chile. AAPG Annual Convention and Exhibition, Calgary.

Dott Jr, R.H., 1963. Dynamics of subaqueous gravity depositional processes. AAPG Bulletin 47, 104–128.

Felletti, F., 2002. Complex bedding geometries and facies associations of the turbiditic fill of a confined basin in a transpressive setting (Castagnola Fm., Tertiary Piedmont Basin, NW Italy). Sedimentology 49, 645–667.

Fildani, A., Cope, T.D., Graham, S.A., Wooden, J.L., 2003. Initiation of the Magallanes foreland basin: Timing of the southernmost Patagonian Andes orogeny revised by detrital zircon provenance analysis. Geology 31, 1081–1084.

Fildani, A., Hessler, A.M., 2005. Stratigraphic record across a retroarc basin inversion: Rocas Verdes–Magallanes basin, Patagonian Andes, Chile. Geological Society of America Bulletin 117, 1596–1614.

Fosdick, J.C., Romans, B.W., Fildani, A., Bernhardt, A., Calderón, M., Graham, S.A., 2011. Kinematic evolution of the Patagonian retroarc fold-and-thrust belt and Magallanes foreland basin, Chile and Argentina, 51 30′ S. Geological Society of America Bulletin 123, 1679–1698.

Gamberi, F., Rovere, M., 2011. Architecture of a modern transient slope fan (Villafranca fan, Gioia basin–Southeastern Tyrrhenian Sea). Sedimentary Geology 236, 211–225. doi:10.1016/j.sedgeo.2011.01.007

Grecula, M., Flint, S., Potts, G., Wickens, D., Johnson, S., 2003. Partial ponding of turbidite systems in a basin with subtle growth-fold topography: Laingsburg-Karoo, South Africa. Journal of Sedimentary Research 73, 603–620.

Haughton, P.D., 1994. Deposits of deflected and ponded turbidityents, currents, Sorbas Basin, southeast Spain. Journal of Sedimentary Research 64.

Hickson, T.A., Lowe, D.R., 2002. Facies architecture of a submarine fan channel–levee complex: the Juniper Ridge Conglomerate, Coalinga, California. Sedimentology 49, 335–362.

Hubbard, S.M., Covault, J.A., Fildani, A., Romans, B.W., 2014. Sediment transfer and deposition in slope channels: Deciphering the record of enigmatic deep-sea

processes from outcrop. Geological Society of America Bulletin 126, 857–871. doi:10.1130/B30996.1

Hubbard, S.M., Fildani, A., Romans, B.W., Covault, J.A., McHargue, T.R., 2010. High-Relief Slope Clinoform Development: Insights from Outcrop, Magallanes Basin, Chile. Journal of Sedimentary Research 80, 357–375. doi:10.2110/jsr.2010.042

Hubbard, S.M., Romans, B.W., Graham, S.A., 2008. Deep-water foreland basin deposits of the Cerro Toro Formation, Magallanes basin, Chile: architectural elements of a sinuous basin axial channel belt: Sinuous deep-water foreland basin axial channel, Chile. Sedimentology 55, 1333–1359. doi:10.1111/j.1365-3091.2007.00948.x

Jobe, Z.R., Bernhardt, A., Lowe, D.R., 2010. Facies and Architectural Asymmetry in a Conglomerate-Rich Submarine Channel Fill, Cerro Toro Formation, Sierra Del Toro, Magallanes Basin, Chile. Journal of Sedimentary Research 80, 1085–1108. doi:10.2110/jsr.2010.092

Jobe, Z.R., Lowe, D.R., Morris, W.R., 2012. Climbing-ripple successions in turbidite systems: depositional environments, sedimentation rates and accumulation times: Climbing ripples deposited by turbidity currents. Sedimentology 59, 867–898. doi:10.1111/j.1365-3091.2011.01283.x

Jobe, Z.R., Sylvester, Z., Howes, N., Pirmez, C., Parker, A., Cantelli, A., Smith, R., Wolinksy, M., O'Byrne, C., Slowey, N., Prather, B., 2016. High-resolution, millennial-scale patterns of bed compensation on a sand-rich intraslope submarine fan, western Niger Delta slope. Geological Society of America Bulletin B31440–1.

Kane, I.A., McCaffrey, W.D., Martinsen, O.J., 2009. Allogenic vs. Autogenic Controls on Megaflute Formation. Journal of Sedimentary Research 79, 643–651. doi:10.2110/jsr.2009.072

Katz, H.R., 1963. Revision of Cretaceous Stratigraphy in Patagonian Cordillera of Ultima Esperanza, Magallanes Province, Chile. AAPG Bulletin 47, 506–524.

Kneller, B., Edwards, D., McCaffrey, W., Moore, R., 1991. Oblique reflection of turbidity currents. Geology 19, 250–252.

Kopriva, B.T., Kim, W., 2015. Coevolution of Minibasin Subsidence and Sedimentation: Experiments. Journal of Sedimentary Research 85, 254–264. doi:10.2110/jsr.2015.24

Li, L., Wang, Y., Xu, Q., Zhao, J., Li, D., 2012. Seismic geomorphology and main controls of deep-water gravity flow sedimentary process on the slope of the northern South China Sea. Science China Earth Sciences 55, 747–757. doi:10.1007/s11430-012-4396-1

Lowe, D.R., 1982. Sediment gravity flows: II Depositional models with special reference to the deposits of high-density turbidity currents. Journal of Sedimentary Research 52.

Macauley, R.V., Hubbard, S.M., 2013. Slope channel sedimentary processes and stratigraphic stacking, Cretaceous Tres Pasos Formation slope system, Chilean Patagonia. Marine and Petroleum Geology 41, 146–162. doi:10.1016/j.marpetgeo.2012.02.004

Malkowski, M.A., Sharman, G.R., Graham, S.A., Fildani, A., 2015. Characterisation and diachronous initiation of coarse clastic deposition in the Magallanes-Austral foreland basin, Patagonian Andes. Basin Research n/a-n/a. doi:10.1111/bre.12150

Mansfield, C.F., 1979. Upper Mesozoic subsea fan deposits in the southern Diablo Range, California: Record of the Sierra Nevada magmatic arc. Geological Society of America Bulletin 90, 1025–1046.

Marchès, E., Mulder, T., Gonthier, E., Cremer, M., Hanquiez, V., Garlan, T., Lecroart, P., 2010. Perched lobe formation in the Gulf of Cadiz: Interactions between gravity processes and contour currents (Algarve Margin, Southern Portugal). Sedimentary Geology 229, 81–94. doi:10.1016/j.sedgeo.2009.03.008

Martinsen, O.J., 1989. Styles of soft-sediment deformation on a Namurian (Carboniferous) delta slope, Western Irish Namurian Basin, Ireland. Geological Society, London, Special Publications 41, 167–177.

Moscardelli, L., Wood, L., 2008. New classification system for mass transport complexes in offshore Trinidad. Basin Research 20, 73–98. doi:10.1111/j.1365-2117.2007.00340.x

Mutti, E., 1992. Turbidite sandstones. Agip Istituto di geologia Universita di Parma, Milan.

Nardin, T.R., 1979. A review of mass movement processes sediment and acoustic characteristics, and contrasts in slope and base-of-slope systems versus canyon-fan-basin floor systems.

Patacci, M., Haughton, P.D.W., Mccaffrey, W.D., 2015. Flow Behavior of Ponded Turbidity Currents. Journal of Sedimentary Research 85, 885–902. doi:10.2110/jsr.2015.59

Pemberton, E.A.L., Hubbard, S.M., Fildani, A., Romans, B., Stright, L., 2016. The stratigraphic expression of decreasing confinement along a deep-water sediment routing system: Outcrop example from southern Chile. Geosphere 12, 114–134. doi:10.1130/GES01233.1

Pickering, K.T., Hiscott, R.N., 1985. Contained (reflected) turbidity currents from the Middle Ordovician Cloridorme Formation, Quebec, Canada: an alternative to the antidune hypothesis. Sedimentology 32, 373–394.

Piper, D.J., Normark, W.R., 1983. Turbidite depositional patterns and flow characteristics, Navy submarine fan, California Borderland. Sedimentology 30, 681–694.

Postma, G., Cartigny, M., Kleverlaan, K., 2009. Structureless, coarse-tail graded Bouma Ta formed by internal hydraulic jump of the turbidity current? Sedimentary Geology 219, 1–6. doi:10.1016/j.sedgeo.2009.05.018

Prather, B.E., Booth, J.R., Steffens, G.S., Craig, P.A., 1998. Classification, lithologic calibration, and stratigraphic succession of seismic facies of intraslope basins, deep-water Gulf of Mexico. AAPG bulletin 82, 701–728.

Prather, B.E., Pirmez, C., Winker, C.D., 2012. Stratigraphy of linked intraslope basins: Brazos-Trinity system western Gulf of Mexico. Application of the Principles of Seismic Geomorphology to Continental-Slope and Base-of-Slope Systems: Case

Studies from Seafloor and Near-Seafloor Analogues: SEPM, Special Publication 99, 83–109.

Prélat, A., Hodgson, D.M., 2013. The full range of turbidite bed thickness patterns in submarine lobes: controls and implications. Journal of the Geological Society 170, 209–214.

Pyles, D.R., Syvitski, J.P.M., Slatt, R.M., 2011. Defining the concept of stratigraphic grade and applying it to stratal (reservoir) architecture and evolution of the slope-to-basin profile: An outcrop perspective. Marine and Petroleum Geology 28, 675–697. doi:10.1016/j.marpetgeo.2010.07.006

Romans, B.W., Fildani, A., Graham, S.A., Hubbard, S.M., Covault, J.A., 2010. Importance of predecessor basin history on sedimentary fill of a retroarc foreland basin: provenance analysis of the Cretaceous Magallanes basin, Chile (50-52°S): Importance of predecessor basin history on sedimentary. Basin Research 22, 640–658. doi:10.1111/j.1365-2117.2009.00443.x

Romans, B.W., Fildani, A., Hubbard, S.M., Covault, J.A., Fosdick, J.C., Graham, S.A., 2011. Evolution of deep-water stratigraphic architecture, Magallanes Basin, Chile. Marine and Petroleum Geology 28, 612–628. doi:10.1016/j.marpetgeo.2010.05.002

Romans, B.W., Hubbard, S.M., Graham, S.A., 2009. Stratigraphic evolution of an outcropping continental slope system, Tres Pasos Formation at Cerro Divisadero, Chile. Sedimentology 56, 737–764. doi:10.1111/j.1365-3091.2008.00995.x

Ross, W.C., Halliwell, B.A., May, J.A., Watts, D.E., Syvitski, J.P.M., 1994. Slope readjustment: A new model for the development of submarine fans and aprons. Geology 22, 511. doi:10.1130/0091-7613(1994)022<0511:SRANMF>2.3.CO;2

Shultz, M.R., Fildani, A., Cope, T.D., Graham, S.A., 2005. Deposition and stratigraphic architecture of an outcroppong ancient slope system: Tres Pasos Formation, Magallanes Basin, southern Chile. Geological Society, London, Special Publications 244, 27–50.

Shultz, M.R., Hubbard, S.M., 2005. Sedimentology, Stratigraphic Architecture, and Ichnology of Gravity-Flow Deposits Partially Ponded in a Growth-Fault-Controlled Slope Minibasin, Tres Pasos Formation (Cretaceous), Southern Chile. Journal of Sedimentary Research 75, 440–453. doi:10.2110/jsr.2005.034

Sinclair, H.D., Cowie, P.A., 2003. Basin-Floor Topography and the Scaling of Turbidites. The Journal of geology 111, 277–299.

Sinclair, H.D., Tomasso, M., 2002. Depositional evolution of confined turbidite basins. Journal of Sedimentary Research 72, 451–456.

Smith, C.H.L., 1977. Sedimentology of the Late Cretaceous (Santonian-Maastrichtian) Tres Pasos Formation, Ultima Esperanza District, southern Chile. University of Wisconsin, Madison, Wisconsin.

Spychala, Y.T., Hodgson, D.M., Flint, S.S., Mountney, N.P., 2015. Constraining the sedimentology and stratigraphy of submarine intraslope lobe deposits using exhumed examples from the Karoo Basin, South Africa. Sedimentary Geology 322, 67–81. doi:10.1016/j.sedgeo.2015.03.013

Stevenson, C.J., Jackson, C.A.-L., Hodgson, D.M., Hubbard, S.M., Eggenhuisen, J.T., 2015. Deep-Water Sediment Bypass. Journal of Sedimentary Research 85, 1058–1081. doi:10.2110/jsr.2015.63

Sumner, E.J., Amy, L.A., Talling, P.J., 2008. Deposit Structure and Processes of Sand Deposition from Decelerating Sediment Suspensions. Journal of Sedimentary Research 78, 529–547. doi:10.2110/jsr.2008.062

Talling, P.J., Masson, D.G., Sumner, E.J., Malgesini, G., 2012. Subaqueous sediment density flows: Depositional processes and deposit types. Sedimentology 59, 1937–2003. doi:10.1111/j.1365-3091.2012.01353.x

Tinterri, R., Muzzi Magalhaes, P., Tagliaferri, A., Cunha, R.S., 2016. Convolute laminations and load structures in turbidites as indicators of flow reflections and decelerations against bounding slopes. Examples from the Marnoso-arenacea Formation (northern Italy) and Annot Sandstones (south eastern France). Sedimentary Geology 344, 382–407. doi:10.1016/j.sedgeo.2016.01.023

Yeilding, C.A., Apps, G.M., 1994. Spatial and temporal variations in the facies associations of depositional sequences on the slope: Examples from the Miocene–Pleistocene of the Gulf of Mexico, in: Submarine Fans and Turbidite Systems: SEPM Foundation, Gulf Coast Section, Fifteenth Annual Research Conference. SEPM, pp. 425–436.

Appendix 1**: Measured Sections.**

Includes all seven sections.

Measured Section 1

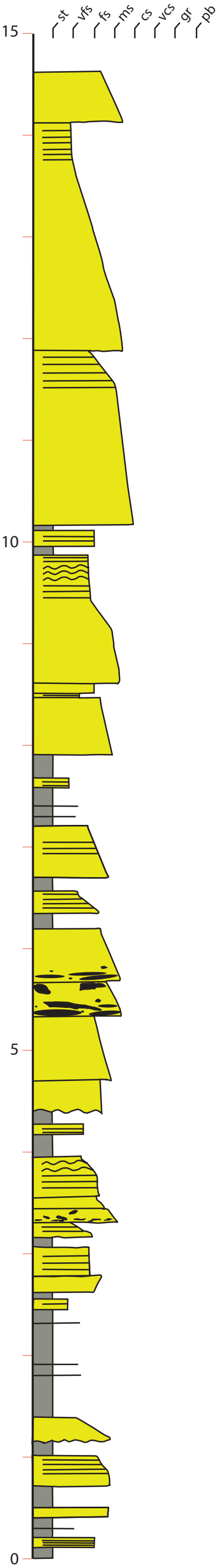

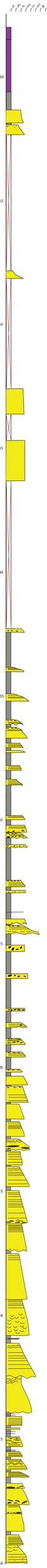
Sandstone
Shale
60
55
50
45
40
35
30
25
20
15
10
5
0

Measured Section 3

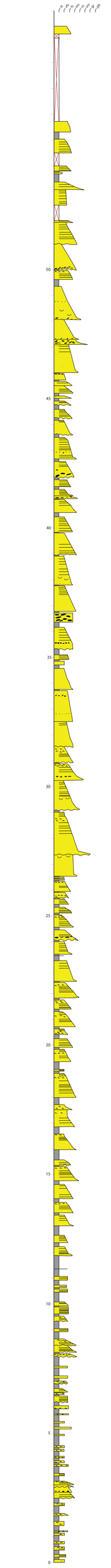

Measured Section 4

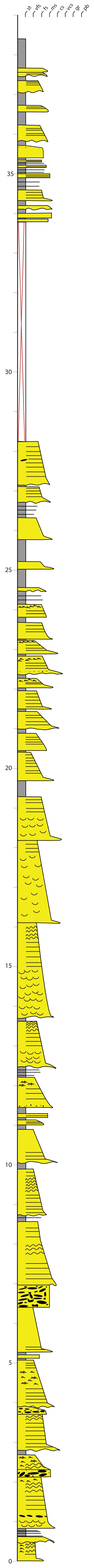

Measured Section 5

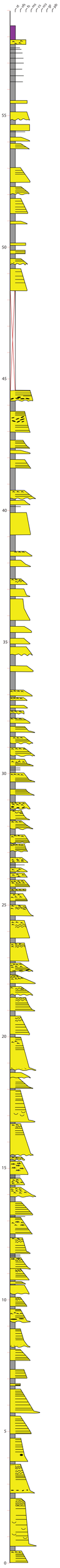

Measured Section 6

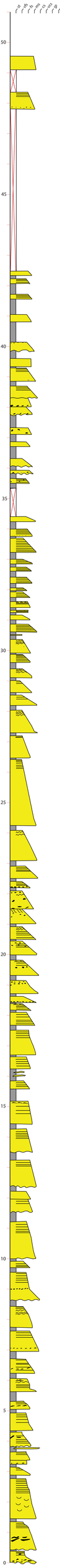

Measured Section 7